2009

Geometric Capacity Studies for DTV Transmitter Identification By Using Kasami Sequences

Xiaoyu Feng
Louisiana State University and Agricultural and Mechanical College, xfeng4@tigers.lsu.edu

GEOMERTIC CAPACITY STUDIES FOR DTV TRANSMITTER IDENTIFICATION BY USING KASAMI SEQUENCE

A Thesis

Submitted to the Graduate Faculty of the
Louisiana State University and
Agricultural and Mechanical College
in partial fulfillment of the
requirements for the degree of
Master of Science in Electrical Engineering

In

The Department of Electrical and Computer Engineering

by
Xiaoyu Feng
B.E., Beijing University of Aeronautics and Astronautics, China, 2007
May 2010

ACKNOWLEDGEMENTS

I would like to thank Louisiana State University for funding this research. I would also like to thank Dr. Hsiao-Chun Wu for guiding me and sharing his wealth of experience and knowledge to further my education. Special thanks go to Dr. Xianbin Wang for his guidance and help with sequence generating and other aspects of this project. Thanks also to Dr. Xue-bin Liang and Dr. Morteza Naraghi-Pour for their involvement in the committee for this thesis. Thanks also to my EE friends, Kun Yan, Lu Lu, Yonas Debessu and Charisma Edwards for their help in general.

TABLE OF CONTENTS

LIST OF TABLES

LIST OF FIGURES

ABSTRACT

The transmitter identification of the DTV systems becomes crucial nowadays. Transmitter identification (TxID, or transmitter fingerprinting) technique is used to detect, diagnose and classify the operating status of any radio transmitter of interest. A pseudo random sequence was proposed to be embedded into the DTV signal before transmission. Thus, the transmitter identification can be realized by invoking the cross-correlation functions between the received signal and the possible candidates of the pseudo random sequences. Gold sequences and Kasami sequences are two excellent candidates for the transmitter ID sequences as they provide a large family of nearly-orthogonal codes. In order to investigate the sensitivity of the transmitter identification in different topologies and Kasami sequences with different length, we present the analysis here for four different geometric layouts, namely circular distribution, doubly concentric and circular distribution, square array and hexagonal tessellation. The covered area and the lowest received signal-to-interference ratio are considered as two essential parameters for the multiple-transmitter identification. It turns out to be that the larger the Kasami sequence length, the larger the received signal-to-interference ratio. Our new analysis can be used to determine the required Kasami sequence length for a specific broadcasting coverage.

1. INTRODUCTION OF CURRENT DIGITAL TERRESTIAL TELEVISION SYSTEMS

1.1 Historical View of DTV

Digital Terrestrial Television (DTV) is a new type of advanced broadcasting technology that can televise videos using the digital signals instead of the analog signals propagated by analog TV. The most significant advantage for switching analog TV to digital TV is that digital TV channels demand less bandwidth. The required bandwidths correspond to the conveyed image quality which depends on the compression level. Therefore, DTV will enable broadcasters to supply televised programs with better picture and sound quality. Meanwhile, multiple programming choices and interactive capabilities can also be facilitated by digital terrestrial broadcasts. However, new equipments and costly antenna installation are necessary a digital TV system is in place. It also increases the electricity consumption and the switching time between channels due to digital receivers.

This switch from analog broadcast television to digital broadcast television is called the digital TV (DTV) transition. The first country which adopted the digital broadcasting systems was Luxembourg, in 2006. The Netherlands, Finland, Andorra, Sweden, Switzerland, Germany and Portugal have made the transition since then. Since November 1998, the DTV services were initiated to cover North America [1]. In the United States, an additional broadcast channel distribution was set up for each broadcast TV station in 1996 so that stations can attempt to carry out digital broadcast while still keeping their analog broadcast channels simultaneously. With special

dispensation, some major full-power broadcast television stations started to broadcast solely on digital airwaves on February 17, 2009. On June 12, 2009, all television stations are projected to stop broadcasting analog signals and to switch to digital signals. All over-the-air signals will be transformed digital and the analog TV transmission will finally disappear in the United States on that day. Several countries, includes China, Japan and the United Kingdom, etc., have been scheduled to make the analog to digital TV transition just in a few years.

The technology and the systems used in the DTV broadcasting vary all over the world. The standards developed by the Advanced Television Systems Committee (ATSC), have been widely adopted in North America and South Korea for DTV transmission. Most European countries, Australia, New Zealand, Colombia, Uruguay and some African countries adopted the DVB-T standards instead. The DTV systems used in China now comply with the DMB-T/H standards while the ISDB-T standard is used in Japan.

1.2 DTV receivers

There are several different approaches for the DTV reception. Three among them are normally used in our daily life. The traditional means of receiving the DTV signals is to establish antennae toward the broadcasting tower nearby. However, the channel accessibility strictly limits the number of TV channels (programs) available to the users. On the other hand, the most two popular ways to receive DTV signals for a board accessibility of channels are via digital satellites and digital cables. Nowadays,

we also can watch DTV programs through mobile devices facilitating the DTV standards such as DMB and DVB-H.

In the United States, the ATSC is the official standard for the DTV transmission and the terrestrial video broadcasting. The ATSC digital television standard, which has been developed by the Advanced Television Systems Committee Technology Group on Distribution (T3), was released in 1995. This standard describes a DTV system designed to transmit high quality video and audio and ancillary data over a single-frequency channel at 6 MHz. Such a system can reliably deliver about 19 Mbps of throughput in each 6-MHz terrestrial broadcasting channel and about 38 Mbps of throughput in each 6-MHz cable television channel. The objective of this standard is to represent the video, audio, and data subject to the high compression ratio while preserving the minimum level of quality required for any specific application.

1.3 DTV System Block Diagram

The block diagram illustrating the DTV transmitter specified by the ATSC standard addressed in Section 1.2 is shown in Figure 1 [2].

The video subsystem and the audio subsystem are employed for source coding and data compression so as to encode the video and audio data in a digital compressed form. The similar compression techniques are also applied for both ancillary data and control data. The purpose of this coder is to greatly reduce the multimedia information to be delivered such that the allocated narrow TV channels can still effectively carry on. The current digital television systems adopt the MPEG-2 video stream syntax for

the video compression and use the Digital Audio Compression (AC-3) standard for the audio compression.

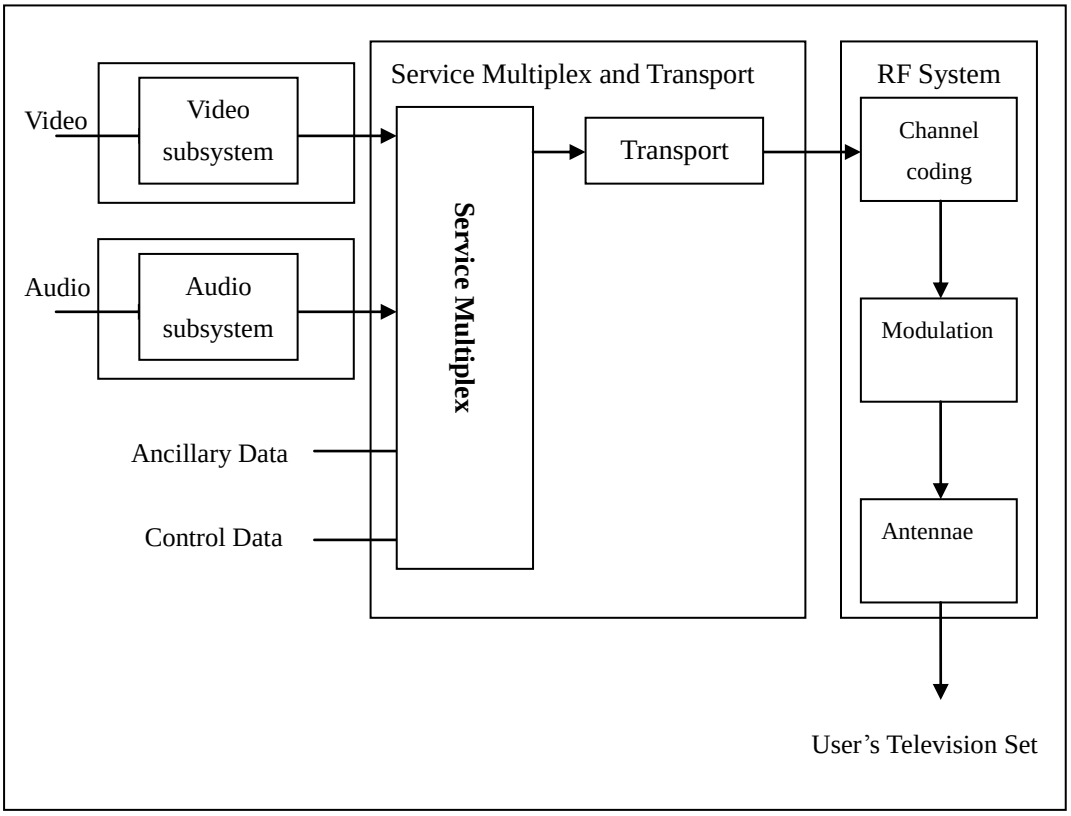

Figure 1－ATSC digital terrestrial television transmitter (broadcasting model).

The service multiplex and transport mechanisms in Figure 1 refers to the functions of dividing the digital data stream, including video, audio and ancillary data, into information packets and multiplexing all kinds of data packets into a single stream after each packet category is identified. The digital television systems adopt the MPEG-2 transport stream syntax for the packetization and the multiplexing of video, audio and ancillary data. The MPEG-2 transport stream syntax was developed for the applications where the channel bandwidth or the recording medium capacity is limited and the requirement for an efficient transport mechanism is paramount. It was

also designed to facilitate the interoperability with the ATM (asynchronous transfer mode) transport mechanism.

The RF (radio frequency) system in Figure 1 is employed for the channel coding and the modulation and the signaling. The channel coder creates the redundant information and embeds it into the bit steam in order to help the receiver to reconstruct the original data from the received signal enduring the channel distortion. The modulation subsystem converts the original data to the transmitted signal of appropriate form. The modulation subsystem in the ATSC standard offers two modes: a terrestrial broadcast mode (8 VSB) and a high data-rate mode (16 VSB).

2. TRANSMITTER IDENTIFICATION TECHNIQUES IN DTV SYSTEM

The transmitter identification of the aforementioned DTV systems becomes crucial nowadays. For example, the identification of ENG (electronic news gathering) crews is very important and necessary for live televised programs. Hence, the transmitter identification techniques are in demand for modern DTV systems. In the following sections, the introduction will be made for the data frame of transmitted DTV signals and the embedded pseudo random sequences.

2.1 Data Frame Structure for DTV Transmission

Transmitter identification (TxID, or transmitter fingerprinting) technique is used to detect, diagnose and classify the operating status of any radio transmitter of interest. In the DTV applications, the transmitter identification refers to the (static or mobile) station identification for the television channels. Due to the rapid development of DTV and the increasing numbers of DTV channels, the need for the television channel identification becomes an urgent issue. As a result, transmitter identification has been recognized as an important feature in the ATSC Synchronization Standard for Distributed Transmission [3].

Figure 2 shows how every data frame is constructed for the DTV signal transmission [2]. According to Figure 2 and [2], a DTV data frame consists of two data fields, each containing 313 data segments. The first segment of each data field is a unique synchronizing signal (Data Field Sync) and includes the training sequence to be used by the equalizer at the receiver. Each of the remaining 312 data segments

carries the data from one 188-byte transport packet plus its associated FEC overhead. The actual data contained in each data segment comes from several transport packets because of data interleaving. Each data segment consists of 832 symbols. The first four symbols are transmitted in binary form to facilitate the segment synchronization data. This Data Segment Sync signal (the four symbols) also represents the sync byte of the 188-byte MPEG-compatible transport packet. The remaining 828 symbols of each data segment carry the remaining 187 bytes of a transport packet and its associated FEC overhead.

2.2 Pseudo Random Sequences Embedded in DTV Signal

In the DTV transmitter identification, the TV station's information is added into the DTV transport data stream and it can be obtained by demodulating the DTV signal. However, successful reception is not always guaranteed due to many reasons in the real scenario. The transmitter ID acquired this way only provides the identification of the transmitter associated with the strongest signal path [3]. Therefore, the identification of a weak source signal is impossible [3]. Hence, a pseudo random sequence was proposed to be embedded into the DTV signal before transmission [3]. Thus, the transmitter identification can be realized by invoking the cross-correlation functions between the received signal and the possible candidates of the pseudo random sequences. The illustration of the DTV signal with injected pseudo random sequences is shown in Figure 3.

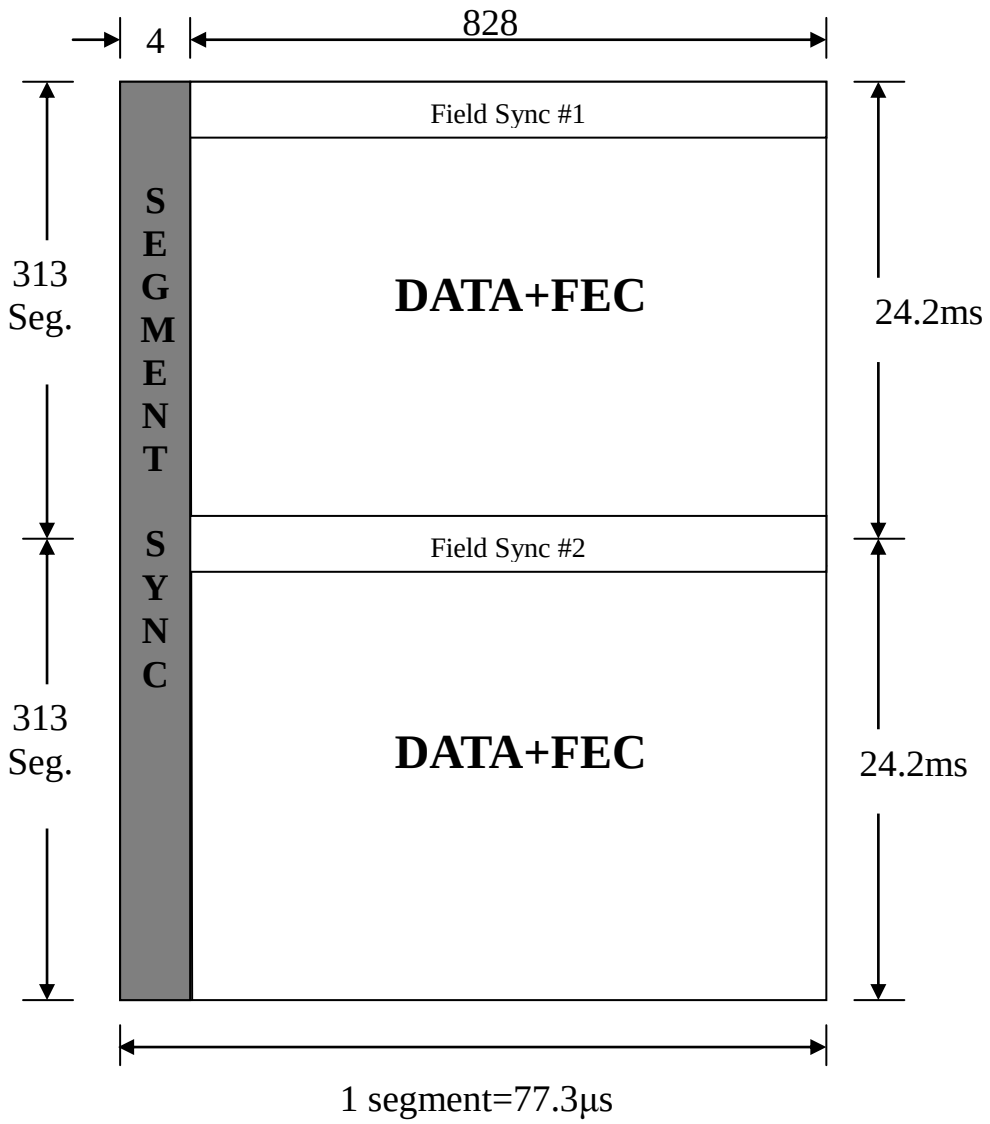

Figure 2−Data frame for the DTV signal transmission (FEC: forward error correction, sync: fields to be used for synchronization).

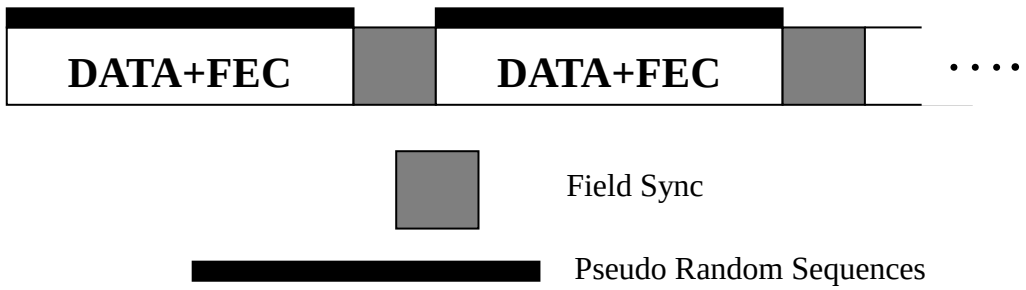

Figure 3−One field of the transmitted ATSC signal embedded with pseudo random sequences.

In this method [3], one essential property of the pseudo random sequences for the transmitter identification is that they are nearly orthogonal to each other. Another important property is that the pseudo random sequence is embedded into the DTV signal in a low power level so that the reception of the DTV signal will not be impacted virtually. Transmitter identification is processed by calculating the cross-correlation function between the received DTV signal and the original embedded pseudo random sequence, which does not depend on the additional resource.

In addition to the two aforementioned essential properties, the size of the pseudo random sequence set also needs to be considered since each sequence can only be used to identify one channel in the world-wide area [3]. Therefore, an enough number of pseudo random sequences must be available in practice.

Gold sequences [4, 5] and Kasami sequences [6, 7] are two excellent candidates for the transmitter ID sequences as they provide a large family of nearly-orthogonal codes. Kasami sequences have period $N = 2^n-1$, where n is a positive even integer. There are two classes of Kasami sequences: the small set and the large set. The large set contains all the sequences belonging to the small set. However, only the small set is optimal in the sense of matching Welch's lower bound for the correlation functions. Although the small set of Kasami sequences can provide the better identification performance than the Kasami sequences from the large set due to their correlational properties, the total number of the pseudo random sequences from the small Kasami set is limited (similar restriction can be found for the Gold sequences). Therefore,

Kasami sequences from the large set are employed as the most desirable pseudo random sequences for the transmitter identification of DTV signals.

3. MATHEMATICAL PROPERTIES OF KASAMI SEQUENCES

As previously discussed in Chapter 2, the Kasami sequences are adopted as the transmitter ID sequences in the modern DTV systems. Hence, we would like to introduce how to generate Kasami sequences and their essential mathematical properties for transmitter ID in the following sections.

3.1 Algebraic Methods for Binary Sequence Construction

Binary sequences are important for spread-spectrum systems, code-division multiple-access (CDMA) systems and broadband satellite communications [8, 9]. Among all binary sequence families, those who have low non-zero-lag autocorrelation values, low cross-correlation values, large family size [10] and large linear span [11] are preferred in practice. These correlation properties are exploited to minimize the interference among the emitted signals so as to facilitate the signal detection even at the low signal-to-noise ratios [12]-[16].

Many binary sequences are built upon the elementary family, namely the maximal-length binary sequences (m-sequences). The m-sequences can be simply represented based on the trace function $tr_m^n(x) \stackrel{\text{def}}{=} \sum_{i=0}^{n-1} x^{2^{mi}}$, where $x \in GF(2^n)$. Since the m-sequences have ideal autocorrelation properties, it is natural to study the cross-correlation function between an m-sequence and its decimations. Many families of low-correlation sequences have been constructed using m-sequences and their decimations [17, 18]. For example, the Gold sequence family [19, 20] was constructed from a pair of m-sequences given by

$$\{tr_1^n(x)\} \text{ and } \{tr_1^n(x^{2^k+1})\}. \quad (1)$$

For an odd *n* and an arbitrary integer *k* with gcd(*n*, *k*)=1.The small set of Kasami sequences can be constructed from

$$\{tr_1^n(x)\} \text{ and } \{tr_1^n(x^{2^{n/2}+1})\} \text{ for even } n. \quad (2)$$

The large set of Kasami sequences can be further extended here [9]. We assume that *n* is even and take *k* to satisfy gcd(*k*, *n*)=2 for odd *n*/2 or gcd(*k*, *n*)=1 for even *n*/2. The three m-sequences

$$\{tr_1^n(x)\}, \{tr_1^n(x^{2^k+1})\} \text{ and } \{tr_1^{n/2}(x^{2^{n/2}+1})\} \quad (3)$$

can be used to obtain the large set of Kasami sequences [9].

The Gold sequence and Kasami sequences both can be constructed by the maximum-length sequences [21]. Often, maximal linear feedback shift registers are used for generating the maximum-length sequences. The resulting sequences are periodic and can be reproduced by the shift registers (i.e., a length-*m* register produces an m-sequence of length 2^m-1). The autocorrelation function of a maximum-length sequence is very similar to a train of Kronecker delta functions. An example of maximum-length sequence generated by a shift register of length 4 is shown in Figure 4.

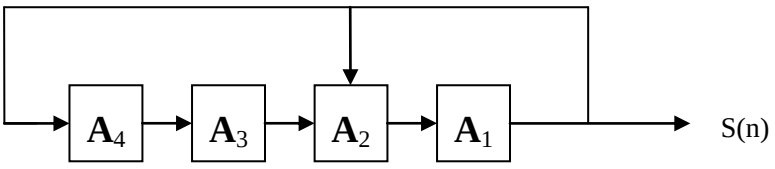

Figure 4−A maximum-length sequence generator of length 4.

The sequence generation illustrated by Figure 4 can be expressed as follows:

$$A_k[n+1] = \begin{cases} A_3[n] + A_1[n], & k = 2 \\ A_{k+1}[n], & \text{otherwise} \end{cases}, \tag{4}$$

where n is the time index, k is the register position, and + represents a modulo-2 addition.

3.2 Correlation Properties of m-sequences, Gold Sequences and Kasami Sequences

The arbitrary pair of m-sequences x_i and x_j lead to a three-valued cross-correlation over a code period $N=2^n-1$, which is given by

$$\rho_{ij}(\tau) = \begin{cases} -1, \\ -t(n), \\ t(n) - 2, \end{cases} \tag{5}$$

where $t(n) \triangleq 2^{(n+2)/2} + 1$. Eq. (5) will serve as the backbone for the correlation properties of Gold sequences and Kasami sequences since the latter families are built upon the m-sequences.

A Gold sequence is produced by the binary addition of two maximum-length sequences which have the same sequence length $N=2^m-1$. Gold sequences take advantage of the fact that, the favorable correlation property of the resulted sequences is guaranteed because only the τ_1- and τ_2-step time-shifting operations and the modulo-2 addition are involved with two distinct m-sequences. Consider every unique combination of (τ_1, τ_2), which can engender a unique Gold sequence. Thus, a large number of distinct Gold sequences can be generated for the communications

applications. However, the Gold sequences possess worse autocorrelation properties than the maximal-length sequences but better cross-correlation properties on the other hand. Similar to Eq. (5), an arbitrary pair of Gold sequences x_i and x_j lead to a three-valued cross-correlation over a code period $N=2^n-1$ [22]:

$$\rho_{ij}(\tau) = \begin{cases} -1, \\ -t(n), \\ t(n)-2, \end{cases} \tag{6}$$

where $t(n) \stackrel{\text{def}}{=} \begin{cases} 2^{(n+1)/2}+1, & \text{if } n \text{ is odd.} \\ 2^{(n+2)/2}+1, & \text{if } n \text{ is even.} \end{cases}$

Besides, Kasami sequences have the similar correlation properties to the Gold sequences since they also arise from the maximum-length sequences. However, the Kasami sequences have an even better cross-correlation property than the Gold sequences. As mentioned in Chapter 2, there are two different sets of Kasami sequences, namely the large set and the small set. For an arbitrary pair of sequences x_i and x_j drawn from the small set of Kasami sequences, the autocorrelation and the cross-correlation over a code period $N=2^n-1$, both can be characterized as the following three-valued function:

$$\rho_{ij}(\tau) = \begin{cases} -1, \\ -s(n), \\ s(n)-2, \end{cases} \tag{7}$$

where $s(n) \stackrel{\text{def}}{=} 2^{n/2}+1$.

Since $|s(n)|<|t(n)|$ according to Eqs. (6) and (7), Kasami sequences have better autocorrelation and cross-correlation properties than Gold sequences. In fact, Kasami sequences have excellent cross-correlation properties because they approach the Welch lower bound [23]. Hence, Kasami sequences are significantly effective for the

transmission identification. Here, the Welch lower bound addresses that the cross-correlation value between any pair of binary sequences in a set consisting of M distinct sequences with the period N is bounded as

$$\phi_{max} \geq N\sqrt{\frac{M-1}{MN-1}}, \tag{8}$$

where ϕ_{max} specifies the maximum magnitude of any cross-correlation value among this set.

The large set of Kasami sequences have a much larger population than that of the small set of Kasami sequences and hence the former can serve for a large capacity of users. The autocorrelation and the cross-correlation for the large set of Kasami sequences over a code period $N=2^n-1$ can be characterized as the following five-valued function:

$$\rho_{ij}(\tau) = \begin{cases} -t(n), \\ -s(n), \\ -1, \\ s(n)-2, \\ t(n)-2, \end{cases} \tag{9}$$

where

$$t(n) \stackrel{\text{def}}{=} 1 + 2^{(n+2)/2}$$

and

$$s(n) \stackrel{\text{def}}{=} \frac{t(n)+1}{2}$$

For example, a 16-bit Kasami sequence drawn from the large set can have the cross-correlation values as -513, -257, -1, 255, and 511 according to Eq. (9). For the auto-correlation values of an n-bit Kasami sequence, we can still employ Eq. (9) to obtain the non-zero-lag values except that we have a constant value of 2^n-1 for the zero-lag autocorrelation. Note that the actual length for an "n-bit Kasami sequence"

should be 2^n-1 due to the name convention by most literature.

The family populations differ from the way of generating Kasami sequences. To generate the small set of Kasami sequences, we begin with a maximal-length sequence s of length $N=2^n$-1 where n is an even integer. A new shorter sequence s' (with length $2^{n/2}$+1) can be formed by sampling every $2^{n/2}$+1 elements of the original sequence s. The resulted sequence s' is periodic with a period of $2^{n/2}$-1 thereby. Then we can generate the small set of Kasami sequences by taking the modulo-2 sum of s with all ($2^{n/2}$-1) cyclic shifts of s' including itself. The collection of all cyclic shifts of s' will form a new sequence of length 2^n-1.To obtain the Kasami sequences of the large set, we also take a maximal-length sequence s of length $N=2^n$-1 where n is an even integer. Similarly, two new shorter sequences s' and s'' can be formed by sampling every $2^{n/2}$+1 and every $2^{(n+2)/2}$+1 elements, respectively. By taking the modulo-2 sum of s with all cyclic shifts of s' and s'', we can generate the large set of Kasami sequences. The family size of the large-set Kasami sequences is $2^{3n/2}$ if n is a multiple of 4 and $2^{3n/2}+2^{n/2}$ if (n mod 4)=2. Note that we express (n mod 4) as $mod_4(n)$ from now on.

The comparison of Gold Sequences, Kasami sequences (small set) and Kasami sequences (large set) is illustrated below.

Note that σ_{max}, ϕ_{max} denote the maximum magnitudes of the autocorrelation and the cross-correlation, respectively

Table I−A COMPARISON OF THE ESSENTIAL FEATURES OF GOLD AND KASAMI SEQUENCES

Sequence	Length (N)	Family Size (M)	σ_{max}	ϕ_{max}
Gold	2^n-1	2^n+1	2^n-1	$2^{(n+1)/2}$+1 if n odd $2^{(n+2)/2}$+1 if n even
Kasami (small set)	2^n-1	$2^{n/2}$	2^n-1	$2^{n/2}$+1
Kasami (large set)	2^n-1	$2^{3n/2}+2^{n/2}$ if $mod_4(n)=2$ $2^{3n/2}$ if $mod_4(n)=0$	2^n-1	$2^{n/2}$+1

3.3 Kasami Sequence generator

Figure 5 illustrates how to generate the large set of Kasami sequences which n=16 in practice. The shift registers are used in the hardware implementation.

The Kasami sequence generator is similar to the Gold sequence generator. The difference between the two generators is that the Kasami sequence generator needs a third sequence generator. In Figure 5, the three preloading (seed) codes, which are set up at the beginning, are circular-shifted and modulo-2 added at some special positions

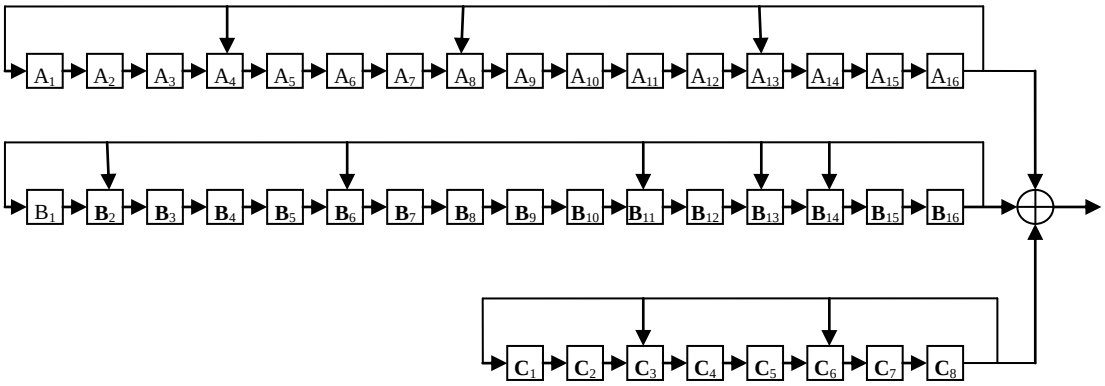

Figure 5−An example of the 16-bit Kasami sequence generator.

in order to generate Kasami sequences. The generated Kasami sequence set is efficient for the transmission identification. In this example, for the large set of Kasami sequences, we have $mod_4(16)=4$ and hence the family size is $2^{3n/2}=2^{24}=16{,}777{,}216$.

A part of a Kasami code generated by the example of Figure 5 is shown below:

1 1 0 0 0 1 0 0 0 0 0 1 0 0 0 1 0 1 1

0 0 0 0 1 0 1 1 0 1 0 1 1 0 0 0 1 1 1

0 1 1 1 0 1 1 0 1 0 0 0 0 1 1 0 0 1 1

1 1 0 1 1 1 0 0 1 1 1 0 0 0 1 1 0 0 0

0 1 1 0 0 0 0 1 0 0 0 0 0 1 0 0 0 1 0

0 1 1 1 1 0 0 0 0 1 1 1 0 1 0 0 0 1 0

0 1 1 0 1 0 0 0 1 1 0 1 1 0 1 0 0 0 1

1 1 0 1 1 0 1 0 0 0 0 1 1 0 0 1 1 0 1

0 0 1 0 1 0 0 1 0 0 0 0 1 1 0 1 0 0 0

1 0 0 1 1 0 0 1 1 1 0 1 0 0 0 1 1 1 0

1 0 0 1 0 0 0 0 1 0 1 1 0 0 0 1 1 0 1

0 0 0 1 1 1 1 1 1 0 0 0 0 1 0 0 0 1 1

1 0 1 0 1 1 0 1 0 0 1 0 0 0 0 0 0 0 1

0 0 1 0 0 0 1 0 1 0 1 1 0 0 0 1 1 1 0

0 0 0 0 1 1 1 1 0 0 1 1 1 0 1 1 0 0 1

0 1 0 0 1 1 1 1 1 1 0 1 0 0 0 0 1 0 1

0 0 0 1 0 0 0 1 1 1 0 0 1 1 0 1 1 0 1

1 1 0 1 1 0 0 0 1 1 0 0 0 0 1 0 0 1 0

0 1 0 1 1 0 0 0 1 0 1 1 1 1 0 1 0 0 0

1 1 1 1 0 1 1 0 0 0 0 0 0 0 1 1 0 0 1

0 1 0 1 1 0 0 0 1 0 0 0 1 0 0 1 0 0 0

1 0 0 1 1 1 0 0 0 1 1 1 1 1 1 0 0 0 0

1 0 1 0 0 1 0 0 0 0 1 1 1 0 1 0 0 0 1

0 0 0 1 1 1 1 0 0 0 0 0 1 1 0 0 0 0 0

1 1 0 0 0 1 0 1 0 0 1 0 0 1 0 1 1 0 0

1 0 1 1 0 1 1 1 1 1 0 0 0 0 1 1 1 1 0

0 1 1 0 1 0 1 1 1 1 0 0 1 0 0 0 0 1 1

0 1 1 0 0 1 1 0 1 0 1 1 1 1 0 0 0 1 1

1 1 0 0 1 1 0 1 1 1 1 1 1 1 0 1 1 1 0

0 1 0 1 1 0 0 1 1 0 0 0 0 1 1 0 1 0 0

0 1 1 0 1 0 0 1 0 1 1 1 0 0 0 0 1 0 1

1 0 0 1 1 1 1 0 1 1 1 1 1 0 0 0 1 0 0

1 0 1 0 1 1 1 0 1 0 0 1 1 1 0 1 0 1 0

1 0 1 1 0 1 1 0 0 1 0 0 1 1 1 1 0 1 1

This subsequence is depicted in Figure 6.

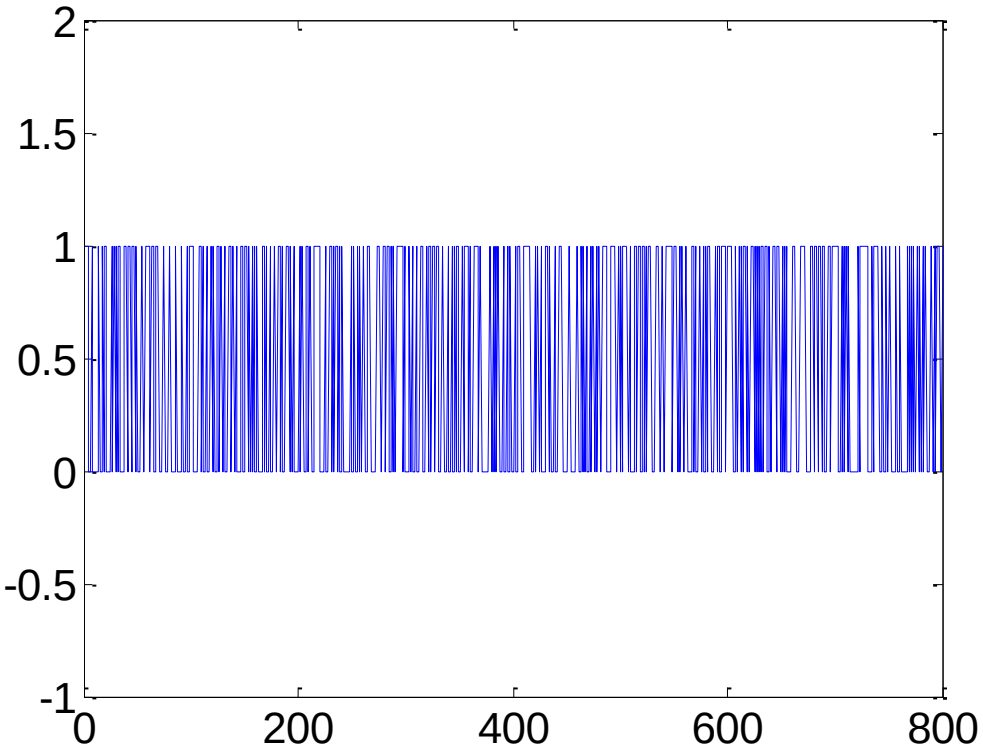

Figure 6−A section of a 16-bit Kasami sequence.

4. STATISTICAL STUDIES OF THE TX-ID USING KASAMI SEQUENCES

Following the discussion in the previous chapters, we would like to study and illustrate the correlation properties for the transmitter identification when the Kasami sequences are adopted for DTV systems. In this thesis, we focus on the large set of Kasami sequences since it will be used in practice. According to Chapter 3, all Kasami sequences are periodic. Hence, we need to study the periodic correlation functions.

In general, the periodic correlation function $R_{i,j}(\tau)$ of the two binary sequences $\{s_i(t)\}$ and $(s_j(t))$ of period 2^n-1 is defined as

$$R_{ij}(\tau) \stackrel{\text{def}}{=} \sum_{t=0}^{2^n-1} (-1)^{s_i(t)-s_j(t+\tau)}. \quad (10)$$

Kasami sequences from the large set as addressed in Chapter 3 are employed for the DTV transmitter identification. We generate an arbitrary 16-bit Kasami sequence and use MATLAB to carry out the normalized autocorrelation function $\frac{R_{ii}(\tau)}{R_{ii}(0)}$, which is depicted in Figure 7. We also generate another 16-bit Kasami sequence to undertake the normalized cross-correlation function $\frac{R_{ij}(\tau)}{\sqrt{R_{ii}(0)R_{jj}(0)}}$ between these two sequences as well, which is depicted in Figure 8.

The significant magnitude difference between the zero-lag autocorrelation value $R_{i,i}(0)$ and other autocorrelation values $R_{i,i}(\tau)$, $\tau \neq 0$ and cross-correlation values $R_{i,j}(\tau)$, $\forall\tau$ are obvious according to Figures 7 and 8. We also plot the cross-correlation function within a small section in Figure 9. It can be verified that the cross-correlation values $R_{i,j}(\tau)$ can only be either -513, -257, -1, 255 or 511.

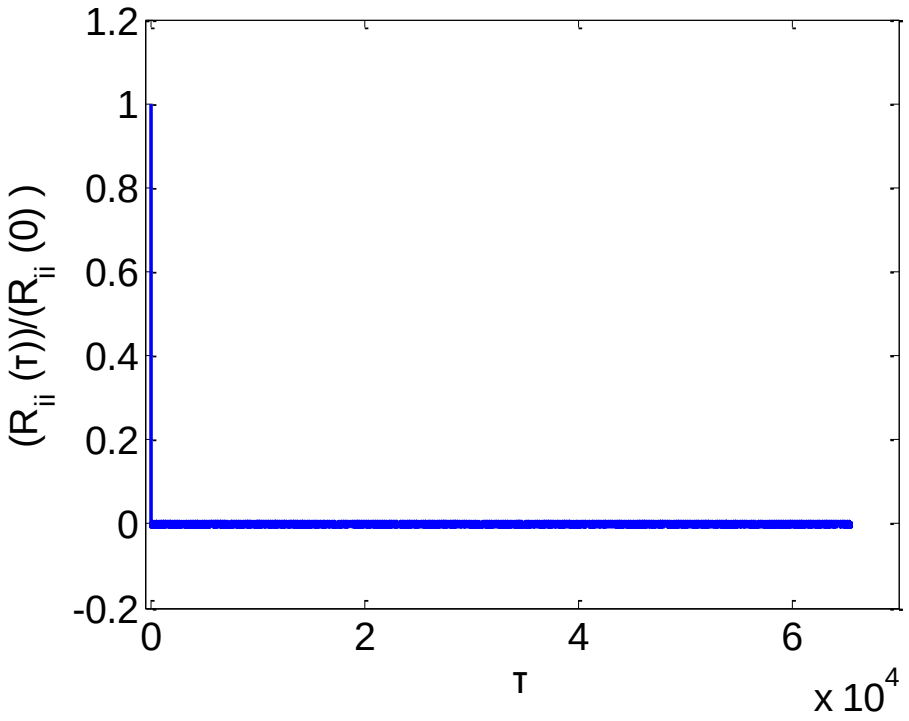

Figure 7−The autocorrelation function of a 16-bit Kasami sequence from the large set (τ is the lag index).

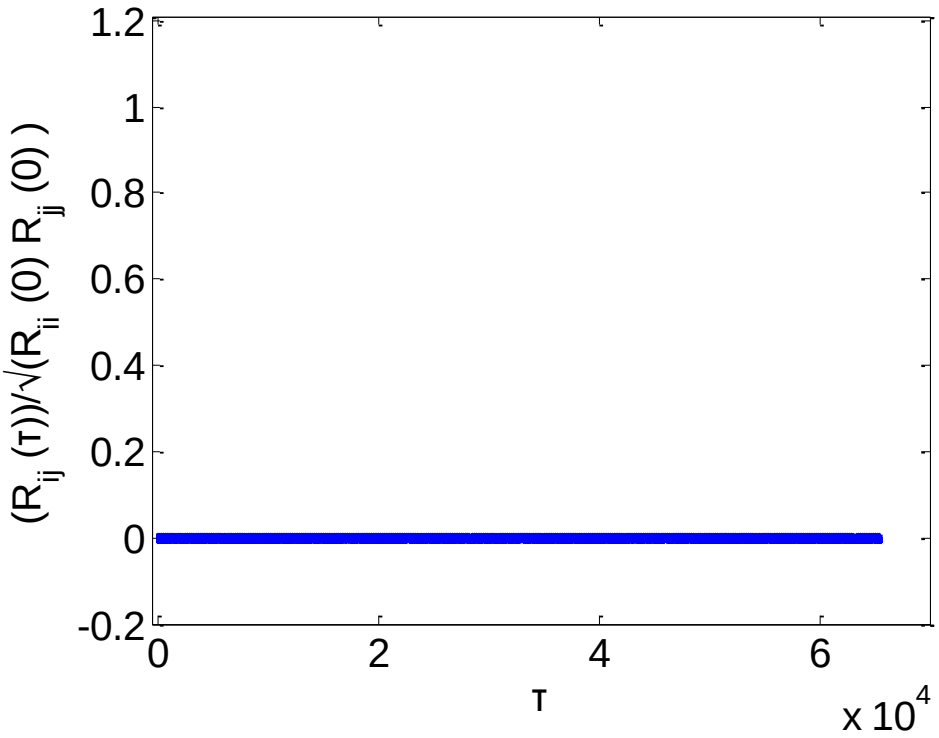

Figure 8−The cross-correlation function of two 16-bit Kasami sequences (τ is the lag index).

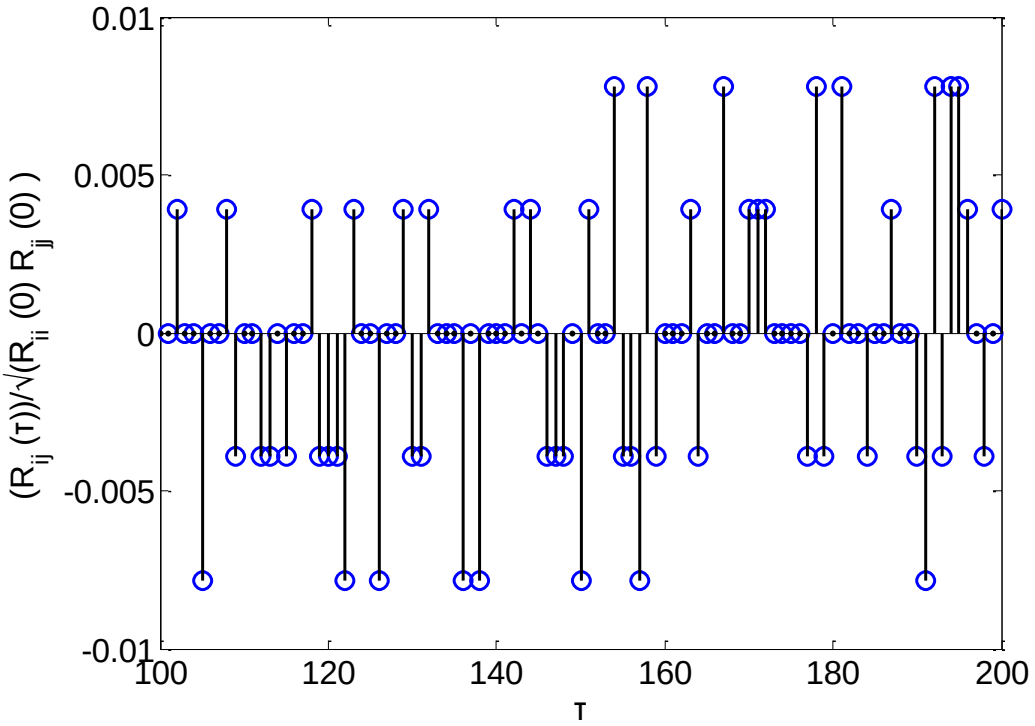

Figure 9−Cross-correlation of two 16-bit Kasami sequences (expanded view).

5. GEOMETRIC STUDIES FOR MULTI-TRANSMITTER IDENTIFICATION USING KASAMI SEQUENCES

In the previous chapters, we introduce the emerging need of the DTV transmitter identification and the adoption of the Kasami sequences mandated by the modern ATSC DTV standards. However, there hardly exists any geometric study on the capacity of the multiple transmitter identification using the Kasami sequences to the best of our knowledge. Hence we would like to dedicate this thesis to address this important issue.

5.1 Introduction of the Geometric Model for DTV Tx-ID

Based on the mathematical properties and the relevant discussion stated in the previous chapters, new geometric studies of the multiple-transmitter-identification using Kasami sequences will be carried out in this chapter. Assume that several DTV signals are sent to one user (or station) simultaneously. The interference and noise need to be considered for the multi-transmitter identification thereby. For example, a television station dispatches several broadcasting vehicles for live news reports. Different DTV signals returned from different vehicles should be identified by the television station. Thus, the geometric model for this scenario is illustrated in Figure 10.

The total number of the transmitters is assumed to be L. Consider the subject transmitter (indexed by k_1) delivers its transmitter ID sequence $s_{k_1}(t)$ to the station. It will be interfered by the signal $s_{k_l}(t)$ sent by another transmitter (indexed by k_l and $l \neq 1$). For simplicity, we further assume that all transmissions occur in the open

area such that no multiple paths exist.

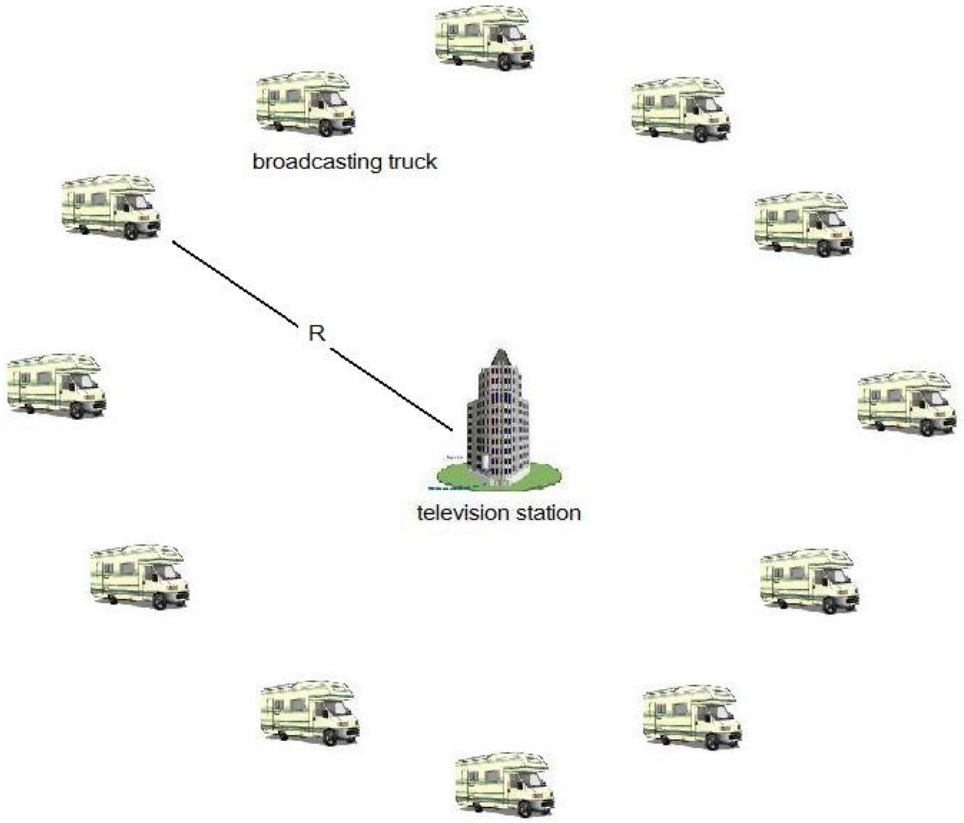

Figure 10−An example of geometric model for multiple-transmitter. identification.

Thus, for each broadcasting truck, the signal-to-interference ratio (SIR) can be defined as

$$SIR = \frac{R_{k_1 k_1}(0)}{\sum_{l=2}^{L} R_{k_1 k_l}(\tau_{1,l})} \tag{11}$$

where both $R_{k_1 k_1}(0)$ and $R_{k_1 k_l}(\tau_l)$ are defined by Eq. (10).

The numerator in Eq. (11) refers to the autocorrelation of the subject broadcasting truck while the denominator refers to the summed cross correlation between the subject transmitter ID sequence and the others.

5.2 Correlation Value of Multiple-Transmitter System

Focused on the scenario given by Section 5.1, we perform the analysis here. From the Monte Carlo simulations, the distributions (histograms) of the multi-transmitter ID cross-correlations (autocorrelations) are illustrated in Figures 11-13 where the horizontal axis refers to the correlation values and the vertical axis refers to the corresponding frequencies to the correlation values.

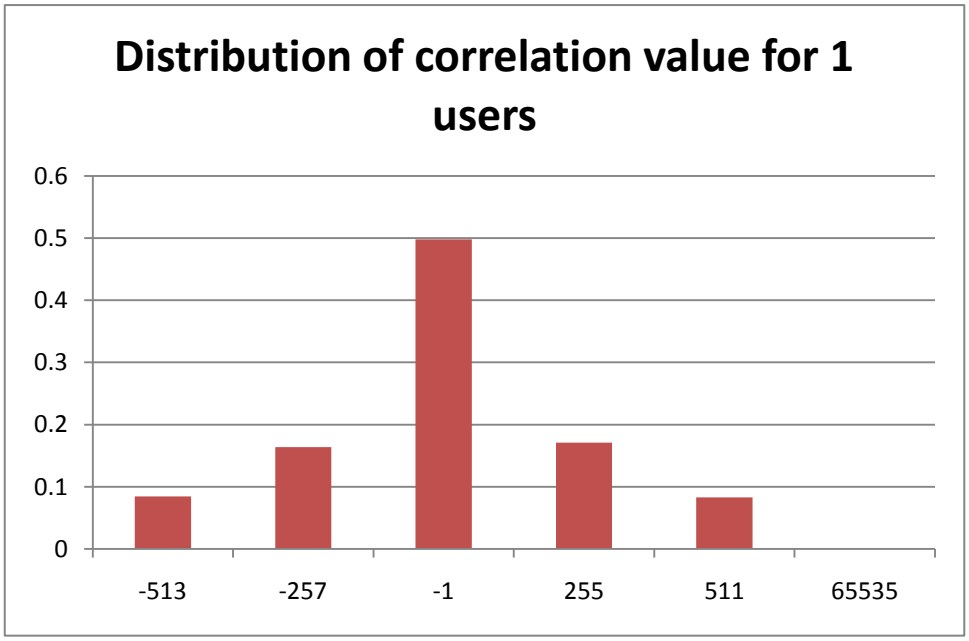

Figure 11−The distribution of the correlation (autocorrelation) values for 1 user.

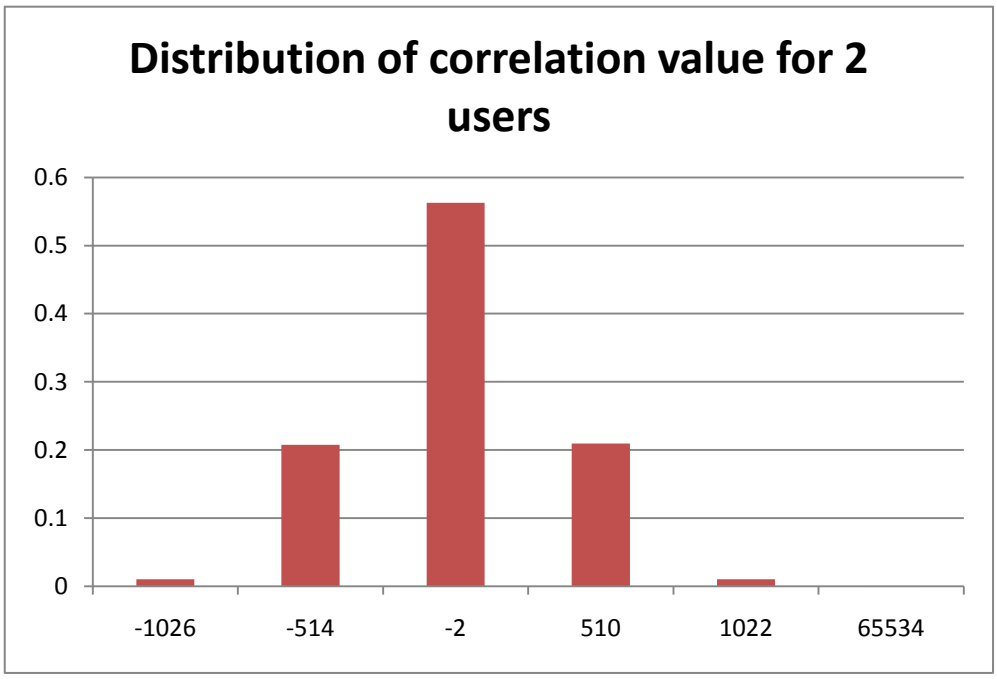

Figure 12−The distribution of the cross-correlation values for 2 users.

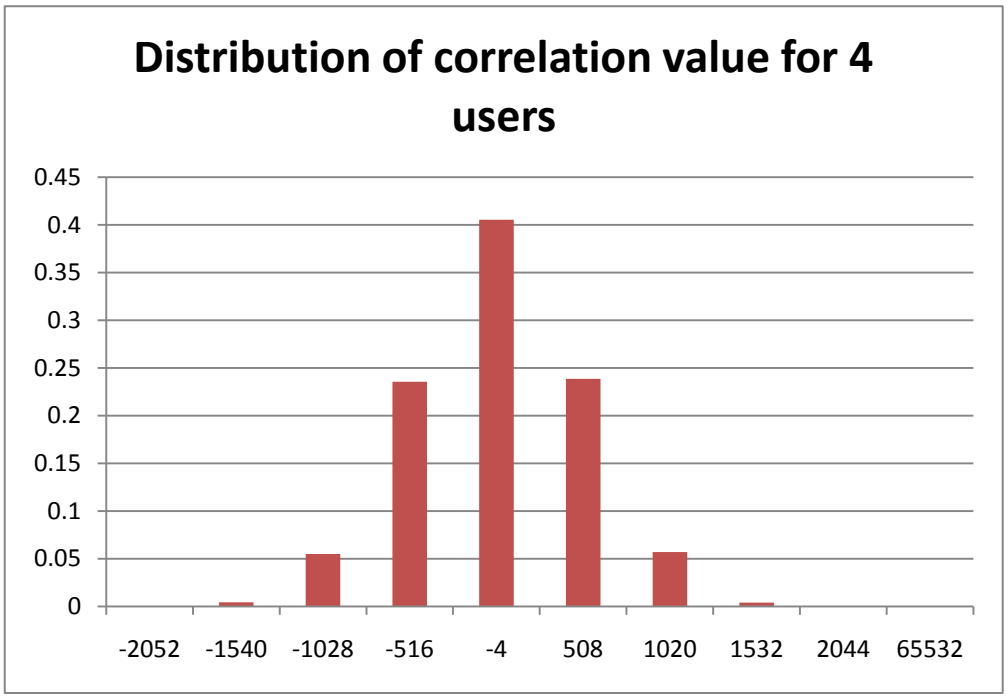

Figure 13−The distribution of the cross-correlation values for 4 users.

5.3 Bounding Analysis of the Signal-to-Interference Ratio for Multiple-Transmitter ID Sequences

According to Eq. (11), we have the following bound for the SIR when the multiple transmitter ID sequences are simultaneously sent, such that

$$\text{SIR} \geq \frac{R_{k_1k_1}(0)}{\sum_{k=2}^{L}\left|R_{k_1k_l}(\tau_{1,l})\right|} = \frac{R_{k_1k_1}(0)}{\left|R_{k_1k_2}(\tau_{1,2})\right| + \left|R_{k_1k_3}(\tau_{1,3})\right| \cdots\cdots + \left|R_{k_1k_L}(\tau_{1,L})\right|} \tag{12}$$

where $\tau_{l,l'}$ specifies the arrival time difference at the base station between the l^{th} and the l'^{th} transmitted ID signals.

For the worst scenario (lowest SIR bound given by Eq. (12)), we set $\left|R_{k_1k_l}(\tau_l)\right|$ as its maximum value $|\text{-}t(n)|=1+2(n+2)/2,\ \forall l$, according the Eq. (9) and set $R_{k_1k_1}(0) = 2^n - 1$ according to Table I. Thus, the inequality in Eq. (12) can be simplified as

$$\text{SIR} \geq \frac{2^n - 1}{(L-1)\cdot\left(1 + 2^{\frac{n+2}{2}}\right)} \tag{13}$$

Note that Eq. (13) can be utilized to measure the geometric capacity for sending multiple TX-ID sequences simultaneously in the same region.

5.4 A Example for 10 Transmitters within a Circular Area

In this subsection, we would like to present a simple example to illustrate the geometric studies of the TX-ID capacity. Assume that there are 10 broadcasting trucks (L=10) sent by the same TV station in the same circular area and the distance between

each broadcasting truck and the TV station is equal to *r* (the radius of this circle), this simple model is shown in Figure 14.

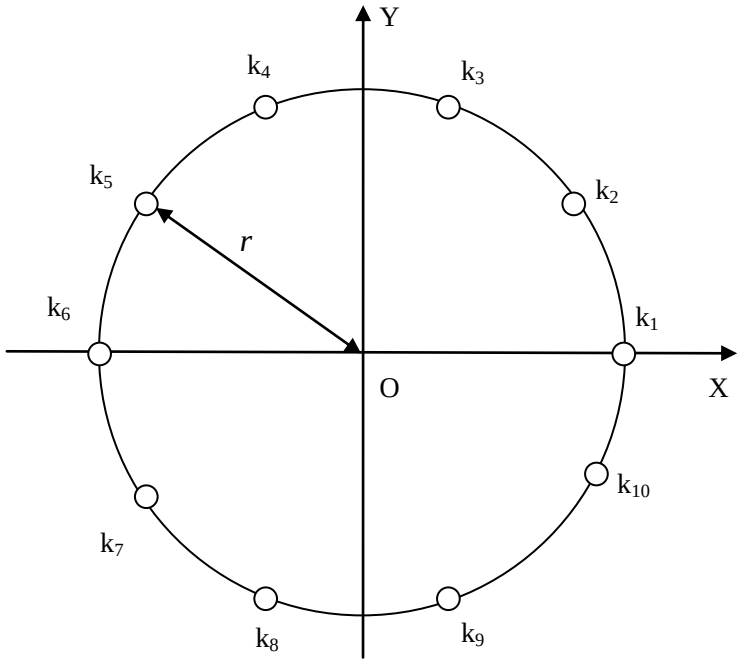

Figure 14−An example of 10 transmitters gathering within a circular area of radius *r*. Small circles denote the transmitters' locations.

According the geometric layout of the multiple transmitters as depicted in Figure 14, Figure 15 illustrates the corresponding relationship between the SIR and the Kasami sequence length according to Eq. (13). Figure 16 demonstrates the same figure as Figure 15 while the SIR is measured in dB instead. Note that the SIR measures are considered at the base station for the primary TX-ID purpose.

A minimum allowable SIR threshold is usually predetermined to guarantee the fidelity of the received TX-ID sequences at the base station. For instance, we take 10 dB as such an SIR threshold in practice. Therefore, for a satisfactory reception of DTV TX-ID signal, the SIR has to be larger than or equal to 10 dB for the reception

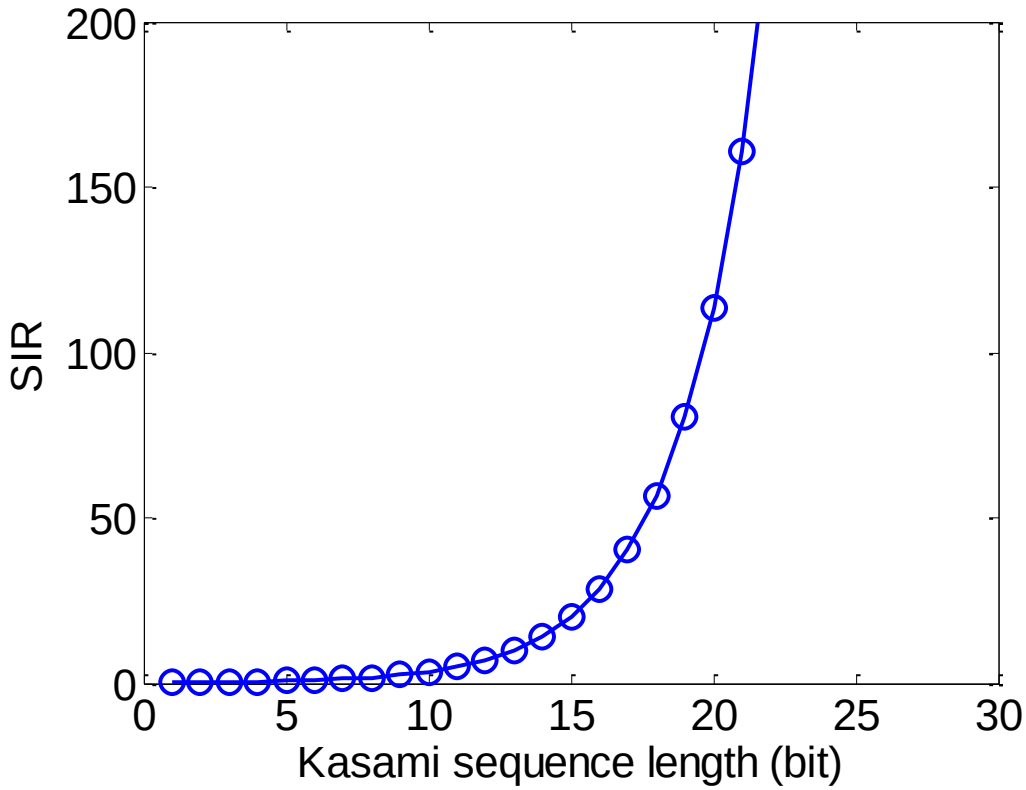

Figure 15−The relationship between the SIR and the Kasami sequence length for the multiple TX layout in Figure 14.

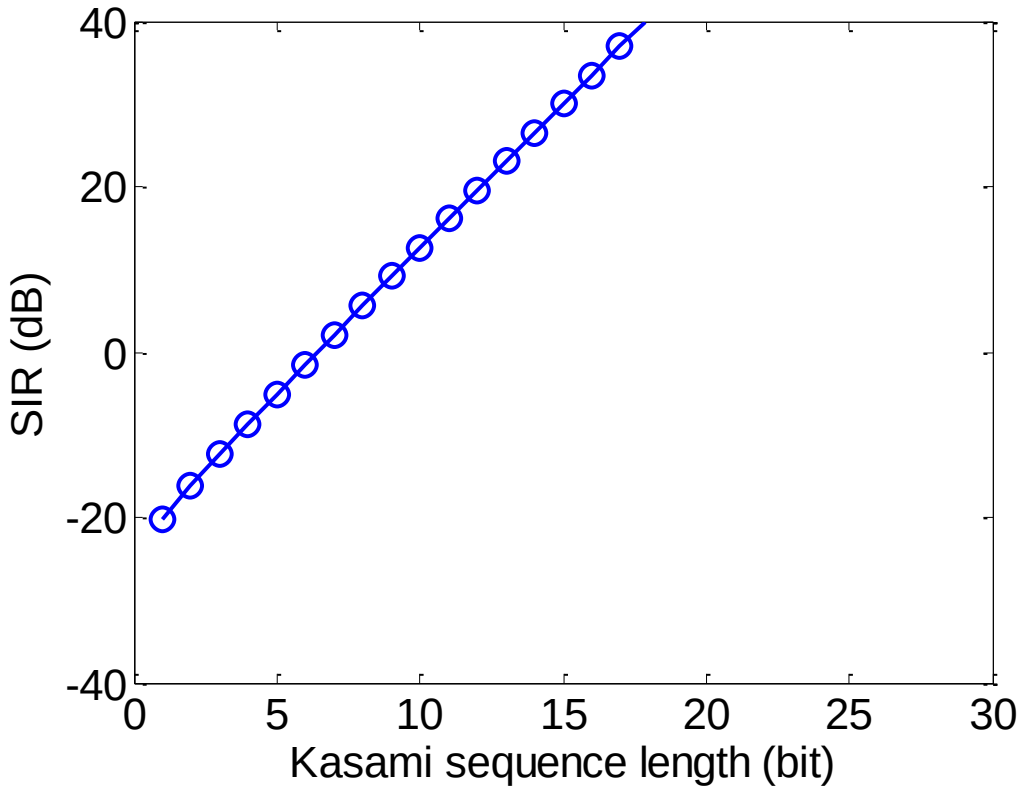

Figure 16−The relationship between the SIR (in dB) and the Kasami sequence length.

of any transmitter ID sequence. Consequently, according to Figure 16, the Kasami sequence length has to be larger than 10 bits. The received SIR is 33.47dB when the Kasami sequence length is 16 bits, which greatly exceeds the minimum required SIR.

5.5 Signal-to-Interference Ratio Analysis for Multiple Tx-ID Transmission with Mobility

Assume that one of the transmitter, say k_l, in Figure 14 moves a distance D away from or toward the origin, where a negative D means that k_l moves into the circle of radius r and a positive D means that k_l moves out of this circle. Based on this mobility, we would like to study the impact on the received SIR of the multiple TX-ID transmission. Figure 17 illustrates this scenario.

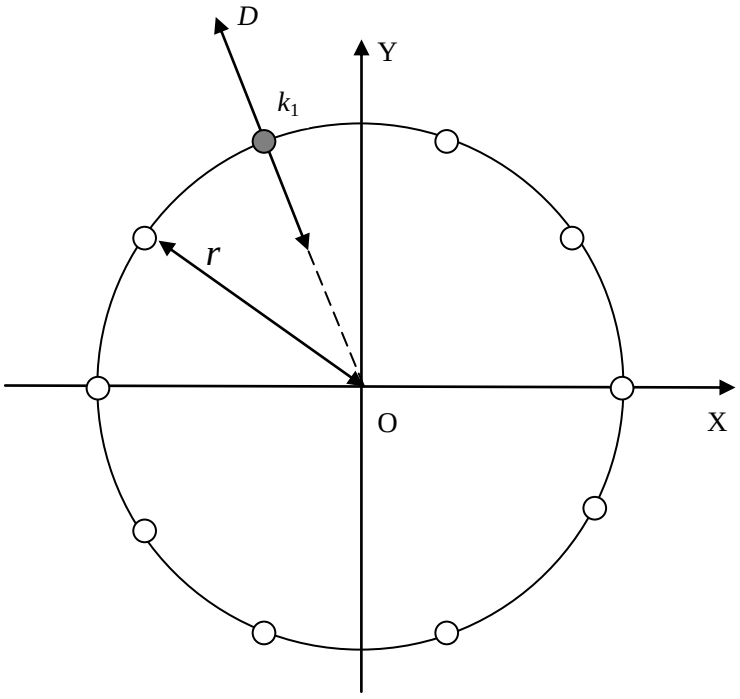

Figure 17−An example of the circularly employed transmitters with some mobility.

Consider that the radius r is significantly larger than the height difference between any transmitter and the base station; one ray model is therefore appropriate

for our discussion. In the one ray model, we assume that is no obstruction between the base station and any transmitter so that each ID signal propagates along a straight line to reach the station. Then the channel model is called line-of-sight (LOS), and the corresponding received signal is called the LOS signal or ray. In this type of LOS channels, the relationship between the transmitted signal power P_t and the received signal power P_r with respect to the distance C between them is characterized as

$$\frac{P_r}{P_t} = \left[\frac{\sqrt{G_l}\lambda}{4\pi C}\right]^2 \tag{14}$$

where $\sqrt{G_l}$ is the product of the transmitting- and receiving-antenna field-radiation patterns along the LOS direction and λ is the signal wavelength [22].

From Eq. (14), we can derive the new expression of SIR when the mobility of a transmitter is addressed. Without loss of generality, we consider that the transmitter k_1 moves and tries to evaluate the SIR for the l^{th} received ID signal associated with the transmitter k_l, which is denoted by SIR_l , l =1, 2, …, L.

For the transmitter k_1, we have

$$\begin{aligned}\text{SIR}_1 &\geq \frac{\frac{1}{(r+D)^2(r+D)^2}R_{k_1k_1}(0)}{\sum_{l=2}^{L}\frac{1}{(r+D)^2r^2}R_{k_1k_l}(\tau_{1,l})} \\ &= \frac{\frac{1}{(r+D)^2}R_{k_1k_1}(0)}{\sum_{l=2}^{L}\frac{1}{r^2}R_{k_1k_l}(\tau_{1,l})} \\ &= \frac{r^2}{(r+D)^2}\frac{R_{k_1k_1}(0)}{\sum_{l=2}^{L}R_{k_1k_l}(\tau_{1,l})}\end{aligned} \tag{15}$$

For any other transmitter k_l $(l \neq 1)$, we have

$$\mathrm{SIR}_l \geq \frac{\frac{1}{r^2 r^2} R_{k_l k_l}(0)}{\frac{1}{(r+D)^2 r^2} R_{k_l k_1}(\tau_{l,1}) + \sum_{l'=2, l' \neq l}^{L} \frac{1}{r^2 r^2} R_{k_l k_{l'}}(\tau_{l,l'})}$$

$$= \frac{\frac{1}{r^2} R_{k_l k_l}(0)}{\frac{1}{(r+d)^2} R_{k_l k_1}(\tau_{l,1}) + \sum_{l'=2, l' \neq l}^{L} \frac{1}{r^2} R_{k_l k_{l'}}(\tau_{l,l'})}$$

$$= \frac{(r+d)^2 R_{k_l k_l}(0)}{r^2 R_{k_l k_1}(\tau_{l,1}) + \sum_{l'=2, l' \neq l}^{L} (r+d)^2 R_{k_l k_{l'}}(\tau_{l,l'})} \tag{16}$$

where $R_{k_l k_{l'}}(\tau_{l'})$) refers to the cross-correlation between the transmitter k_l and a transmitter other than k_1.

Consider the worst SIR scenario and choose the Kasami ID sequence of n bits according to Eqs. (12), (13), SIR_l , l =1, 2, …, L, can be expressed as

$$\mathrm{SIR}_l \geq \begin{cases} \frac{r^2}{(r+D)^2 (L-1)} \frac{2^n - 1}{1 + 2^{\frac{n+2}{2}}}, & l = 1 \\ \frac{(r+D)^2}{[r^2 + (L-2)(r+D)^2]} \frac{2^n - 1}{1 + 2^{\frac{n+2}{2}}}, & l \neq 1 \end{cases}. \tag{17}$$

where L is the total number of the transmitters and n is the bit-length of the Kasami ID sequences

Let's take an example here to illustrate Eq. (17). If $SIR_l \geq 10\,\mathrm{dB}$, $\forall l$ are required, when L=10 and n=16, the range of D is given by

$$-0.5423\, r \leq D \leq 0.1914\, r \tag{18}$$

Therefore, the allowable moving area for the transmitter k_1 to achieve $SIR_l \geq 10\mathrm{dB}$, $\forall l$ is shown in Figure 18.

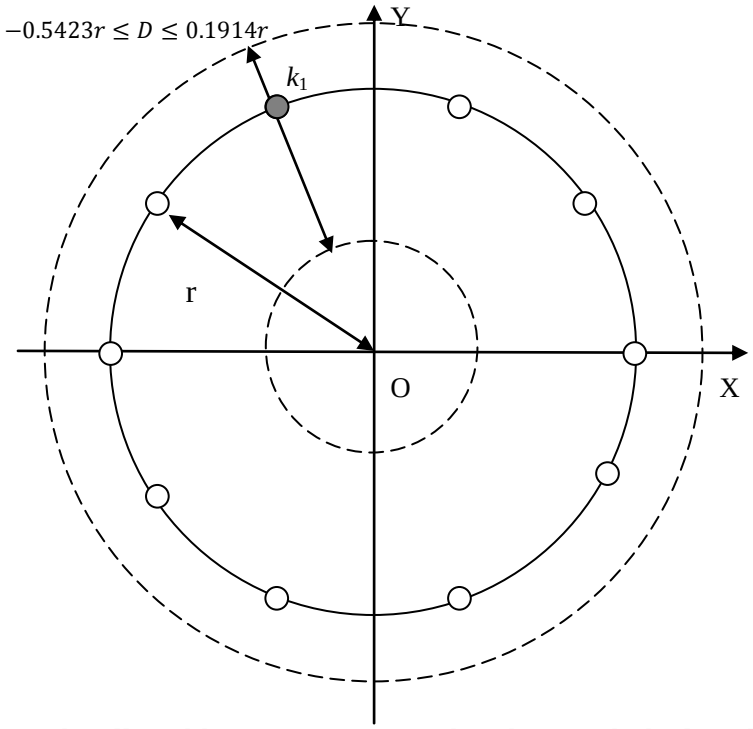

Figure 18−The allowable moving area (within the two dashed circles) for the transmitter k_1 to achieve $\mathrm{SIR}_l \geq 10\mathrm{dB},\ \forall l$.

5.6 Signal-to-Interference Ratio Analysis for Multiple Tx-ID Transmission Subject to Different Topologies

In order to investigate the sensitivity of the transmitter identification in different topologies, we present the analysis here for four different geometric TX layouts, namely (*i*) circular distribution, (*ii*) doubly concentric and circular distribution, (*iii*) square array and (*iv*) hexagonal tessellation. They are discussed in the following subsections.

5.6.1 ID Transmission by Circularly Distributed Transmitters

Similar to Section 5.5, the circularly distributed transmitters (L=16) transmitters as depicted in Figure 19 and 16-bit Kasami sequences from the large set are considered in this example (Scenario I). In this section, d is always defined as the

distance from the station to the nearest transmitter. Hence, *d* is the radius in Figure 19.

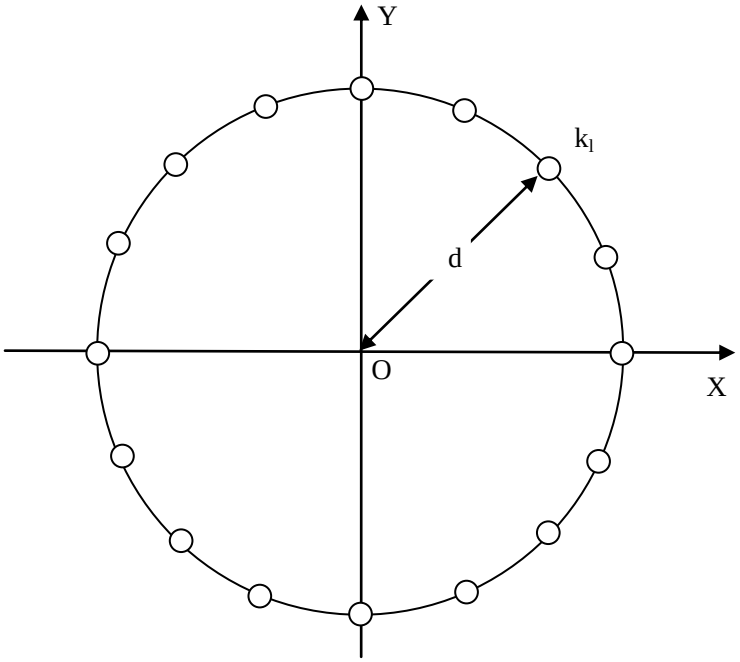

Figure 19−The transmitters are circularly distributed (Scenario I).

From Figure 19, we can find that the received SIRs for all transmitters are the same. In Scenario I, for any transmitter k_l, we have

$$\text{SIR} \geq \frac{\frac{1}{d^2}\frac{1}{d^2}R_{k_l k_l}(0)}{15 \cdot \frac{1}{d^2}\frac{1}{d^2}R_{k_l k_{l'}}(\tau_{l,l'})} = \frac{R_{k_l k_l}(0)}{15 \cdot R_{k_l k_{l'}}(\tau_{l,l'})} \tag{19}$$

where $R_{k_l k_{l'}}(\tau_{l'})$ indicates the cross-correlation values between the different Kasami ID sequences which arrive at the base station.

For the worst situation, we set $R_{k_l k_{l'}}(\tau_{l,l'})$ as its maximum absolute value $|-t(n)|=1+2^{(n+2)/2}$ and $R_{k_l k_l}(0)$ equals to 2^n -1 for n=16. Thus, we have the lower bound of any received SIR as

$$SIR_l \geq 8.5167, \ \forall l. \tag{20}$$

5.6.2 ID Transmission by Doubly and Concentrically Circularly Distributed Transmitters

A more complex topology can be shown in Figure 20 (Scenario II).

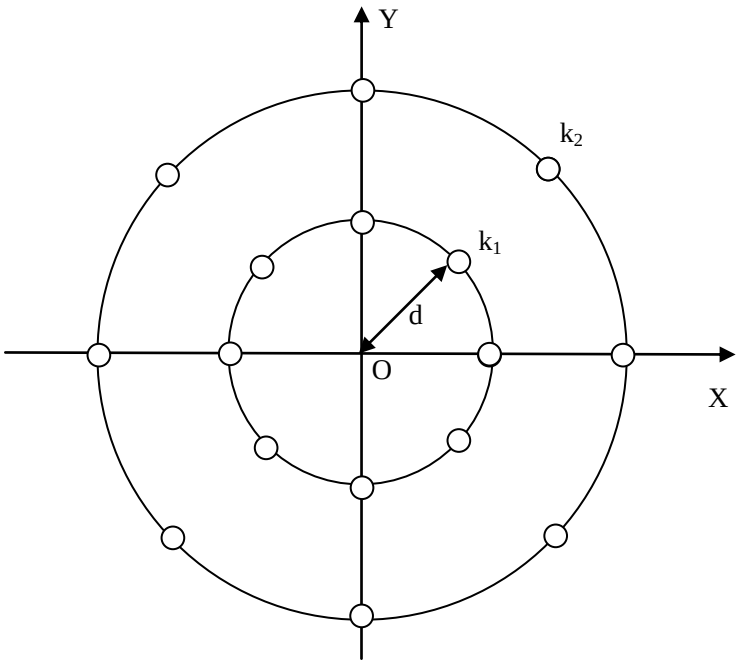

Figure 20−The transmitters are doubly- and concentrically-circularly distributed (Scenario II).

From Figure 20, we only need to consider two different sets of transmitters. Within each individual set, the received SIRs for all transmitters perform the isotropic property. Two arbitrary transmitters (k_1, k_2), each from an individual set, can be considered for the SIR analysis and they are illustrated in Figure 20. Note that $R_{k_l k_{l'}}(\tau_{l'})$ indicates the cross-correlation value between two different Kasami sequences corresponding to the transmitters k_l and $k_{l'}$. Consequently, for the any transmitter k_1 along the inner circle as depicted in Figure 20, we get

$$\mathrm{SIR}_1 \geq \frac{\frac{1}{d^2}\frac{1}{d^2}R_{k_1k_1}(0)}{7\cdot\frac{1}{d^2}\frac{1}{d^2}R_{k_1k_l}(\tau_{1,l}) + 8\cdot\frac{1}{d^2}\frac{1}{4d^2}R_{k_1k_{l'}}(\tau_{1,l'})}$$

$$\geq \frac{R_{k_1k_1}(0)}{9 \cdot R_{k_1k_l}^{max}}$$

(21)

where

$$R_{k_1k_l}^{max} = \max_{l,l',\tau_l}\{|R_{k_1k_l}(\tau_{1,l})|, |R_{k_1k_{l'}}(\tau_{1,l'})|\} \ \forall\, l, l'.$$

For the any transmitter k_2 along the outer circle as depicted in Figure 20, we get

$$SIR_2 \geq \frac{\frac{1}{4d^2}\frac{1}{4d^2}R_{k_2k_2}(0)}{8 \cdot \frac{1}{4d^2}\frac{1}{d^2}R_{k_2k_l}(\tau_{2,l}) + 7 \cdot \frac{1}{4d^2}\frac{1}{4d^2}R_{k_2k_{l'}}(\tau_{2,l'})}$$

$$\geq \frac{\frac{1}{16}R_{k_2k_2}(0)}{(2+\frac{7}{16})R_{k_2k_l}^{max}}.$$

(22)

where

$$R_{k_2k_l}^{max} = \max_{l,l',\tau_l}\{|R_{k_2k_l}(\tau_{2,l})|, |R_{k_2k_{l'}}(\tau_{2,l'})|\} \ \forall\, l, l'$$

For the worst situation, we set $R_{k_1k_l}^{max} = R_{k_2k_l}^{max} = |-t(n)| = 1 + 2^{(n+2)/2}$, and $R_{k_1k_1}(0) = R_{k_2k_2}(0) = 2^n - 1$ for n=16.

The SIR values for the transmitters k_1 and k_2 on the inner and outer circles, which are denoted by SIR_1 and SIR_2 respectively, are bounded as

$$SIR_1 \geq 14.1945, \quad (23)$$

$$SIR_2 \geq 3.2757 \quad (24)$$

5.6.3 ID Transmission by an Array of Transmitters

Now we consider another example where the transmitters are distributed in an

array as depicted in Figure 21. Similar to the discussion in Section 5.6.2, we can categorize the transmitters into three isotropic groups. Within each group, we can arbitrarily pick up a transmitter to evaluate the received SIR for representing all other peer transmitters. For instance, three represented transmitters (k_1, k_2, k_3), each from an individual group, are illustrated in Figure 21.

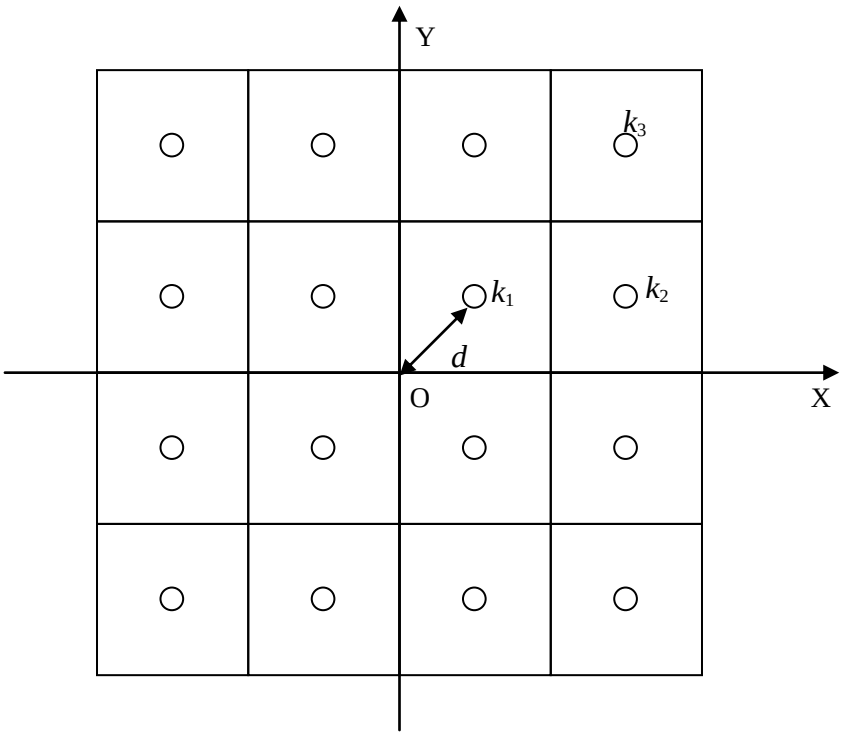

Figure 21−The transmitters are distributed in an array (Scenario III).

For any transmitter k_1 from Group 1, we get

$$\mathrm{SIR}_1 \geq \frac{\frac{1}{d^2}\frac{1}{d^2}R_{k_1k_1}(0)}{3\cdot\frac{1}{d^2}\frac{1}{d^2}R_{k_1k_l}(\tau_{1,l}) + 8\cdot\frac{1}{d^2}\frac{1}{5d^2}R_{k_1k_{l'}}(\tau_{1,l'}) + 4\cdot\frac{1}{d^2}\frac{1}{9d^2}R_{k_1k_{l''}}(\tau_{1,l''})}$$

$$\geq \frac{R_{k_1k_1}(0)}{(3+\frac{8}{5}+\frac{4}{9})R_{k_1k_l}^{max}}. \quad (25)$$

where $R_{k_1k_l}^{max}$=max$\{|R_{k_1k_l}(\tau_{1,l})|, |R_{k_1k_{l'}}(\tau_{1,l'})|, |R_{k_1k_{l''}}(\tau_{1,l''})|\}$ $\forall\, l, l', l''$.

For any transmitter k_2 from Group 2, we can bound its SIR as

$$\begin{aligned}\mathrm{SIR}_2 &\geq \frac{\frac{1}{5d^2}\frac{1}{5d^2}R_{k_2k_2}(0)}{4\cdot\frac{1}{5d^2}\frac{1}{d^2}R_{k_2k_l}(\tau_{2,l})+7\cdot\frac{1}{5d^2}\frac{1}{5d^2}R_{k_2k_{l'}}(\tau_{2,l'})+4\cdot\frac{1}{5d^2}\frac{1}{9d^2}R_{k_2k_{l''}}(\tau_{2,l''})} \\ &\geq \frac{\frac{1}{25}R_{k_2k_2}(0)}{(\frac{4}{5}+\frac{7}{25}+\frac{4}{45})R_{k_2k_l}^{max}}.\end{aligned} \tag{26}$$

where $R_{k_2k_l}^{max}$=max$\{|R_{k_2k_l}(\tau_l)|, |R_{k_2k_{l'}}(\tau_{l'})|, |R_{k_2k_{l''}}(\tau_{l''})|\}$ $\forall\, l, l', l''$.

Finally, for any transmitter k_3 from Group 3, we can bound the corresponding SIR as

$$\begin{aligned}\mathrm{SIR}_3 &\geq \frac{\frac{1}{9d^2}\frac{1}{9d^2}R_{k_3k_3}(0)}{4\cdot\frac{1}{9d^2}\frac{1}{d^2}R_{k_3k_l}(\tau_{3,l})+8\cdot\frac{1}{9d^2}\frac{1}{5d^2}R_{k_3k_{l'}}(\tau_{3,l'})+3\cdot\frac{1}{9d^2}\frac{1}{9d^2}R_{k_3k_{l''}}(\tau_{3,l''})} \\ &\geq \frac{\frac{1}{81}R_{k_3k_3}(0)}{(\frac{4}{9}+\frac{8}{45}+\frac{3}{81})R_{k_3k_l}^{max}}\end{aligned} \tag{27}$$

where $R_{k_3k_l}^{max}$=max$\{|R_{k_3k_l}(\tau_{3,l})|, |R_{k_3k_{l'}}(\tau_{3,l'})|, |R_{k_3k_{l''}}(\tau_{3,l''})|\}$ $\forall\, l, l', l''$.

For the worst situation, we set $R_{k_1k_l}^{max} = R_{k_2k_l}^{max} = R_{k_3k_l}^{max} = |-t(n)| = 1 + 2^{(n+2)/2}$,

and $R_{k_1k_1}(0) = R_{k_2k_2}(0) = R_{k_3k_3}(0) = 2^n - 1$ for n=16.

According to (25)-(27), we can have the numerical bounds for the SIRs of the transmitters belonging to each individual group as

$$\mathrm{SIR}_1 \geq 25.3250, \tag{28}$$

$$\mathrm{SIR}_2 \geq 4.3717, \tag{29}$$

$$\mathrm{SIR}_3 \geq 2.3923. \tag{30}$$

5.6.4 ID Transmission by a Hexagonal Tessellation of Transmitters

The scenario Ⅳ has this kind of topological distribution and the Figure 22 is shown as below.

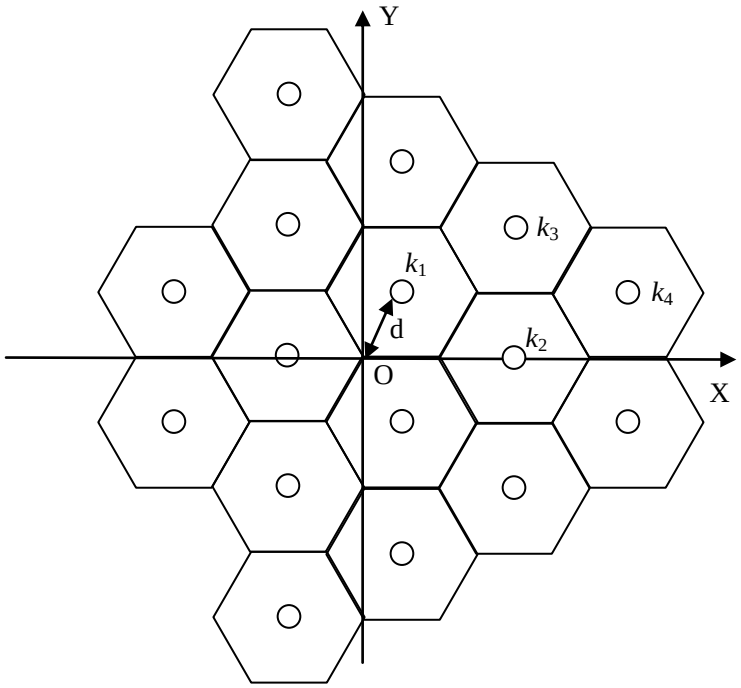

Figure 22−The transmitters are distributed in a hexagonal tessellation (Scenario IV).

Finally, we consider a topology depicted in Figure 22. From Figure 22, four isotropic groups of transmitters can be categorized similarly. We denote the transmitter indices (k_1, k_2, k_3, k_4), each drawn from an individual group, are illustrated in Figure 22.

For any transmitter k_1 from Group 1, we get

$$\mathrm{SIR}_1 \geq \frac{\frac{1}{d^2}\frac{1}{d^2}R_{k_1k_1}(0)}{2\cdot\frac{1}{d^2}\frac{1}{d^2}R_{k_1k_l}(\tau_{1,l})+3\cdot\frac{1}{d^2}\frac{1}{4d^2}R_{k_1k_{l'}}(\tau_{1,l'})+6\cdot\frac{1}{d^2}\frac{1}{7d^2}R_{k_1k_{l''}}(\tau_{1,l''})+4\cdot\frac{1}{d^2}\frac{2}{25d^2}R_{k_1k_{l'''}}(\tau_{1,l'''})}$$

$$\geq \frac{R_{k_1k_1}(0)}{(2+\frac{3}{4}+\frac{6}{7}+\frac{8}{25})R_{k_1k_l}^{max}} \tag{31}$$

where $R_{k_1k_l}^{max}=\max\{|R_{k_1k_l}(\tau_{1,l})|, |R_{k_1k_{l'}}(\tau_{1,l'})|, |R_{k_1k_{l''}}(\tau_{1,l''})|, |R_{k_1k_{l'''}}(\tau_{1,l'''})|\}$

$\forall\, l, l', l'', l'''$.

For any transmitter k_2 from Group 2, we get

$$\mathrm{SIR}_2 \geq \frac{\frac{1}{4d^2}\frac{1}{4d^2}R_{k_2k_2}(0)}{3\cdot\frac{1}{4d^2}\frac{1}{d^2}R_{k_2k_l}(\tau_{2,l})+2\cdot\frac{1}{4d^2}\frac{1}{4d^2}R_{k_2k_{l'}}(\tau_{2,l'})+6\cdot\frac{1}{4d^2}\frac{1}{7d^2}R_{k_2k_{l''}}(\tau_{2,l''})+4\cdot\frac{1}{4d^2}\frac{2}{25d^2}R_{k_2k_{l'''}}(\tau_{2,l'''})}$$

$$\geq \frac{\frac{1}{16}R_{k_2k_2}(0)}{(\frac{3}{4}+\frac{1}{8}+\frac{3}{14}+\frac{2}{25})R_{k_2k_l}^{max}} \tag{32}$$

where $R_{k_2k_l}^{max}=\max\{|R_{k_2k_l}(\tau_{2,l})|, |R_{k_2k_{l'}}(\tau_{2,l'})|, |R_{k_2k_{l''}}(\tau_{2,l''})|, |R_{k_2k_{l'''}}(\tau_{2,l'''})|\}$

$\forall\, l, l', l'', l'''$.

For any transmitter k_3 from Group 3, we get

$$\mathrm{SIR}_3 \geq \frac{\frac{1}{7d^2}\frac{1}{7d^2}R_{k_3k_3}(0)}{3\cdot\frac{1}{7d^2}\frac{1}{d^2}R_{k_3k_l}(\tau_{3,l})+3\cdot\frac{1}{7d^2}\frac{1}{4d^2}R_{k_3k_{l'}}(\tau_{3,l'})+5\cdot\frac{1}{7d^2}\frac{1}{7d^2}R_{k_3k_{l''}}(\tau_{3,l''})+4\cdot\frac{1}{7d^2}\frac{2}{25d^2}R_{k_3k_{l'''}}(\tau_{3,l'''})}$$

$$\geq \frac{\frac{1}{49}R_{k_3k_3}(0)}{(\frac{3}{7}+\frac{3}{28}+\frac{5}{49}+\frac{8}{175})R_{k_3k_l}^{max}} \tag{33}$$

where $R_{k_3k_l}^{max}=\max\{|R_{k_3k_l}(\tau_{3,l})|, |R_{k_3k_{l'}}(\tau_{3,l'})|, |R_{k_3k_{l''}}(\tau_{3,l''})|, |R_{k_3k_{l'''}}(\tau_{3,l'''})|\}$

$\forall\, l, l', l'', l'''$.

For any transmitter k_4, we can bound its SIR as

$$\mathrm{SIR}_4 \geq \frac{\frac{2}{25d^2}\frac{2}{25d^2}R_{k_4k_4}(0)}{3\cdot\frac{2}{25d^2}\frac{1}{d^2}R_{k_4k_l}(\tau_{4,l})+3\cdot\frac{2}{25d^2}\frac{1}{4d^2}R_{k_4k_{l'}}(\tau_{4,l'})+6\cdot\frac{2}{25d^2}\frac{1}{7d^2}R_{k_4k_{l''}}(\tau_{4,l''})+3\cdot\frac{2}{25d^2}\frac{2}{25d^2}R_{k_3k_{l'''}}(\tau_{4,l'''})}$$

$$\geq \frac{\frac{4}{625}R_{k_4k_4}(0)}{(\frac{6}{25}+\frac{3}{50}+\frac{12}{175}+\frac{12}{625})R_{k_4k_l}^{max}} \tag{34}$$

where $R_{k_4k_l}^{max}=\max\{|R_{k_4k_l}(\tau_{4,l})|, |R_{k_4k_{l'}}(\tau_{4,l'})|, |R_{k_4k_{l''}}(\tau_{4,l''})|, |R_{k_4k_{l'''}}(\tau_{4,l'''})|\}$

$\forall\, l, l', l'', l'''$.

For the worst situation, we set $R_{k_1k_l}^{max}=R_{k_2k_l}^{max}=R_{k_3k_l}^{max}=R_{k_4k_l}^{max}=|-t(n)|=1+2^{(n+2)/2}$, and $R_{k_1k_1}(0)=R_{k_2k_2}(0)=R_{k_3k_3}(0)=R_{k_4k_4}(0)=2^n-1$ for n=16.

According to (31)-(34), we can bound the received SIRs for each group as

$$\mathrm{SIR}_1 \geq 32.5301, \tag{35}$$

$$\mathrm{SIR}_2 \geq 6.8284, \tag{36}$$

$$\mathrm{SIR}_3 \geq 3.8146, \tag{37}$$

$$\mathrm{SIR}_4 \geq 2.1085. \tag{38}$$

Assume that the radius for the coverage area by every broadcasting truck is d. The analytic SIR results for different topologies are given in Table II. According to Table II, we depict the relationships between the covered area and the lowest received SIR (absolute value or dB value) in Figures 23, 24.

Table II−THE ANALYTIC SIR RESULTS FOR DIFFERENT TOPOLOGIES (n=16)

Scenario	Covered area	The lowest SIR	The lowest SIR(dB)
Ⅰ	12.57 d^2	8.52	9.30
Ⅱ	28.27d^2	3.28	5.15
Ⅲ	32 d^2	2.39	3.79
Ⅳ	41.57d^2	2.11	3.24

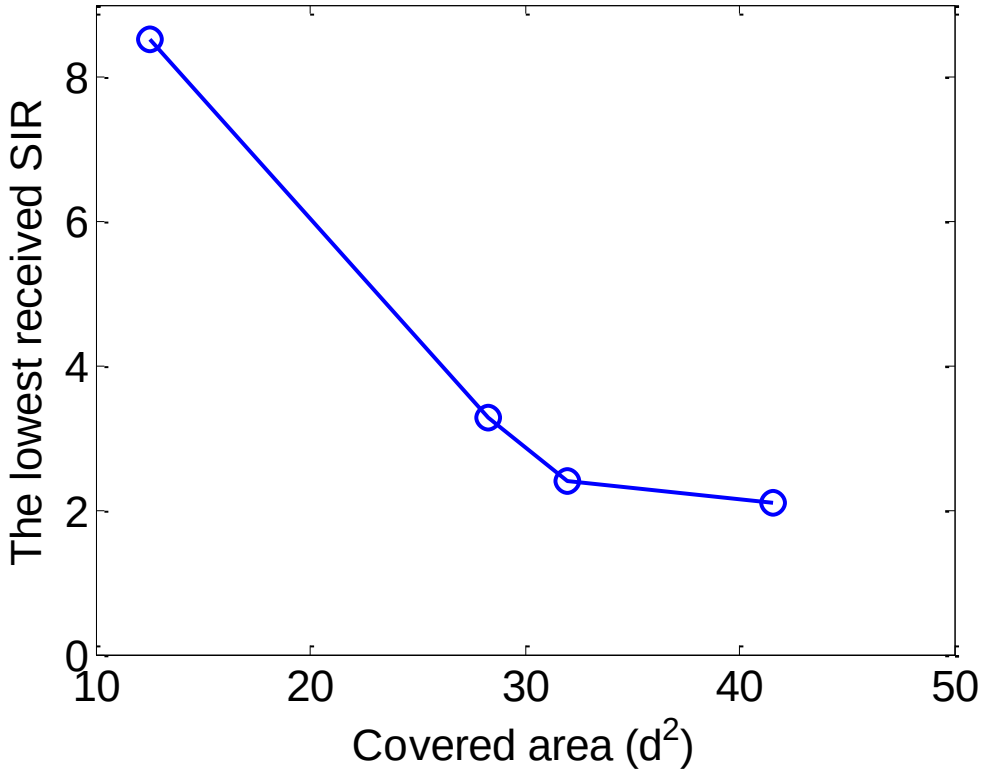

Figure 23−The relationship between the covered area and the lowest received SIR.

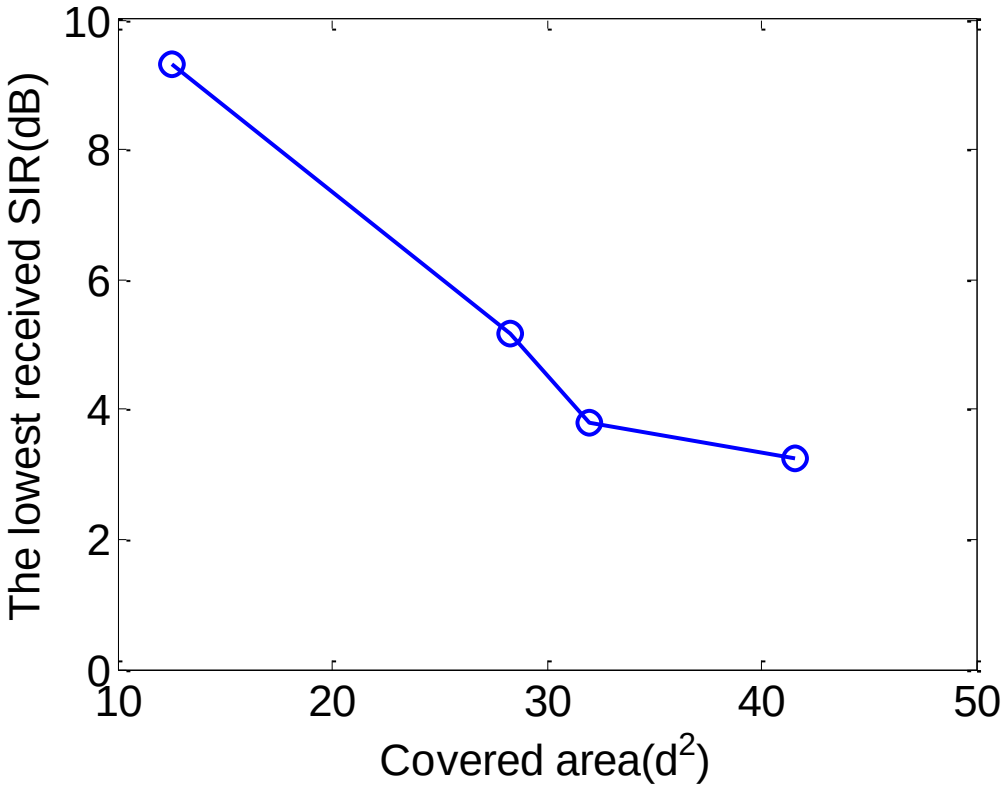

Figure 24− The relationship between the covered area and the lowest received SIR (in dB).

5.7 Comparative Studies for Different Kasami Sequence Lengths

Now we vary the Kasami sequence length (n=14, 18) to follow Section 5.6 for the SIR analysis again. Different scenarios described in Section 5.6 are also considered here. Tables III, IV list the analytic SIR results for these four topologies when the Kasami sequence lengths are n=14 and n=18.

We also depict the relationships between the covered area and the lowest received SIR (absolute value or dB value) for three different Kasami sequence lengths. According to Tables III, IV, and Figures 25, 26, we can find that the larger the Kasami sequence length, the larger the received SIR. However, the receiver processing time

Table III－THE ANALYTIC SIR RESULTS FOR DIFFERENT TOPOLOGIES (n=14)

Scenario	Covered area	The lowest SIR	The lowest SIR(dB)
Ⅰ	12.5664 d^2	4.2498	6.2837
Ⅱ	28.2743d^2	1.6345	2.1338
Ⅲ	32 d^2	1.1938	0.7693
Ⅳ	41.5692 d^2	1.0521	0.2206

Table IV THE ANALYTIC SIR RESULTS FOR DIFFERENT TOPOLOGIES (n=18)

Scenario	Covered area	The lowest SIR	The lowest SIR(dB)
Ⅰ	12.5664 d^2	17.0500	12.3172
Ⅱ	28.2743d^2	6.5577	8.1675
Ⅲ	32 d^2	4.7893	6.8027
Ⅳ	41.5692 d^2	4.2210	6.2542

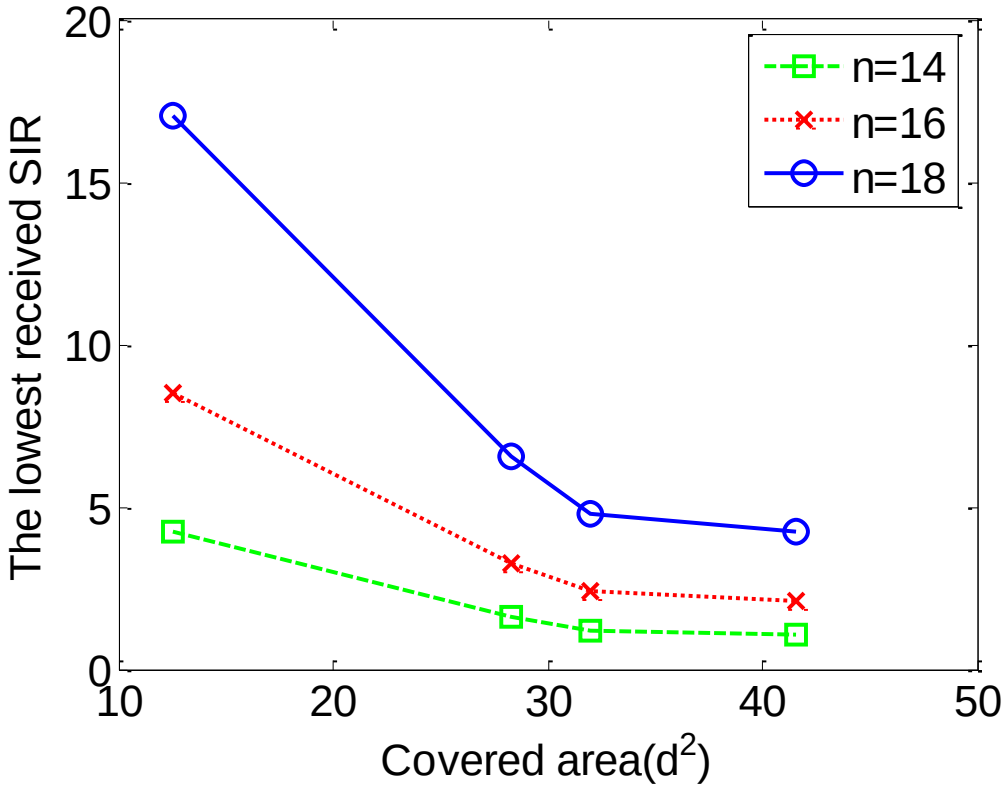

Figure 25−The relationship between the covered area and the lowest received SIR for three different Kasami sequence lengths.

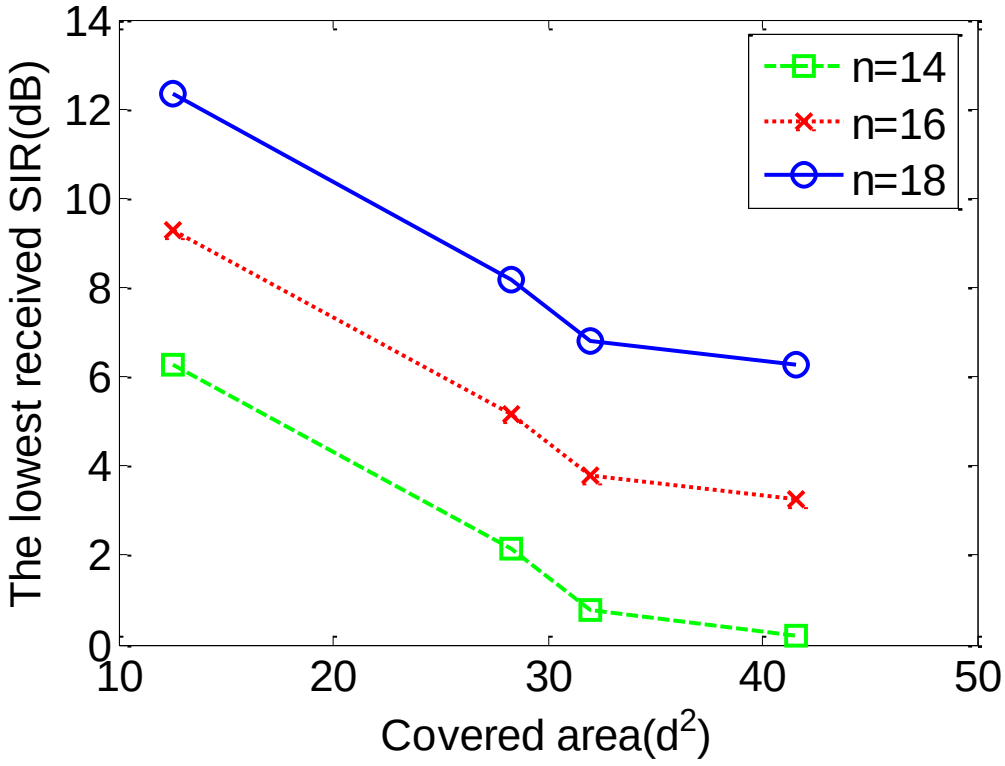

Figure 26−The relationship between the covered area and the lowest received SIR (in dB) for three different Kasami sequence lengths.

and complexity both are proportional to the ID sequence length and there should be some trade-off to seek.

CONCLUSION

The multiple-transmitter identification in digital terrestrial television systems has been studied in this thesis. According to the ATSC standard, the Kasami sequences are adopted as the embedded ID sequences due to its excellent correlation properties compared to other pseudo random sequences. We employ the crucial mathematical properties of the Kasami sequences and evaluate the received signal-to-interference ratio measures at the base station for the transmitted ID signals.

On the other hand, different topologies are investigated for the transmitter ID signal quality at the base station. The covered area and the lowest received signal-to-interference ratio are considered as two essential parameters for the multiple-transmitter identification. It turns out to be that the larger the Kasami sequence length, the larger the received signal-to-interference ratio. Our new analysis can be used to determine the required Kasasmi sequence length for a specific broadcasting coverage.

REFERENCES

[1] Y. Wu, X. Wang, R. Citta, B. Ledoux, ,S. Lafleche, and B. Caron, "An ATSC DTV receiver with improved robustness to multipath and distributed transmission environments," *IEEE Transactions in Broadcasting*, vol. 50, no.1, pp.32-41, March.2004.

[2] ATSC *Digital Television Standard*, September 16, 1995.

[3] X. Wang, Y. Wu, and B. Caron, "Transmitter Identification Using Embedded Pseudo Random Sequences," *IEEE Transactions on Broadcasting*, vol. 50, no.3, pp. 244-252, September 2004.

[4] W. W. Peterson and E.J. Weldon, *Error-correction Codes*, 2nd ed:MIT press,1972

[5] R. E. Ziemer and R. L. Peterson, *Digital Communication and Spread Spectrum Systems*: Macmillan, 1985.

[6] T. Kasami, "Weight distribution formula for some class of cyclic codes," *Technology Report* ,no. R-285, University of Illinois, 1966.

[7] D.V. Sarwate and M.B. Pursley, "Cross correlation properties of pseudorandom and related sequences," *IEEE proceedings*, vol.68, Issue: 5 , pp. 593-619, May 1980.

[8] M. K. Simon, J. K. Omura, R. A. Scholtz, and B. K. Levitt, *Spread Spectrum Communications Handbook*, McGraw-Hill, 2001

[9] X. Zeng, J. Liu, L. Hu, "Generalized Kasami Sequences: The Large Set," *IEEE Transactions on Information Theory*, vol. 53, no. 7, pp. 2587-2598, July 2007.

[10] T. Helleseth and P. V. Kumar, "Sequences with low correlation," *in Handbook of Coding Theory,* V. S. Pless and W. C. Huffman Eds. Amsterdam, The Netherlands: Elsevier Science, vol. 2, 1998.

[11] X. Zeng, L. Hu, Q. Liu, Y. Zhu, "Binary Sequences with Optimal Correlations and Large Linear Span," *Communications, 2006 IEEE International Conference*, vol.1, June 2006, pp. 385-390.

[12] A. Chow, "Performance of spreading Codes for direct sequence code division multiple access (DS-CDMA)," *Technical Report*, Stanford University, 2003.

[13] J. D. H. White and R. E. Challis, "A Golay sequencer based NDT system for highly attenuating materials," *IEE Colloquium on Noncontacting and Remote NDT*, London, UK ,1992, pp. 7/1-7/7.

[14] S. Z. Budisin, B. M. Popovic and I. M. Indjin, "Designing radar signals using complementary sequences," Radar – 87, Proceedings of the International Conference, London, England, October, 1987, pp.593-597.

[15] J. Jorg K.-W. and M. Berg, "Sophisticated mobile robot sonar sensing with pseudo-random codes," *Robotics and Autonomous Systems*, vol. 25, no.3-4, pp. 241-251, November 1998.

[16] M. Hazas and A. Ward, "A high performance privacy-oriented location system," in *Proceedings of the 1st IEEE International Conference on Pervasive Computing and Communications (PerCom 2003)*, Dallas, USA, March 2003, pp. 216-223.

[17] T. Helleseth, C. Ding, T. Helleseth, and H. Niederreiter, Eds., "Correlation of m-sequences and related topics," *in Proceedings of SETA'98,Discrete Math. Theoretical Computer Science*, pp. 49-66, London, October 1999.

[18] H.M. Trachtenberg, "On the cross-correlation functions of maximal linear recurring sequences," Ph.D. Dissertation, University of Southern California, Los Angeles, CA, 1970.

[19] R. Gold, "Optimal binary sequences for spread spectrum multiplexing," *IEEE Transactions on Information Theory*, vol.13, issue:4 , pp. 619-621, October1967.

[20] R. Gold, "Maximal recursive sequences with 3-valued recursive cross correlation functions," *IEEE Transactions on Information Theory*, vol. 14, issue:1, pp. 154-156, January 1968.

[21] S. W. Golomb, "Shift Register Sequences," Holden-Day, San Francisco, 1967.

[22] A. Goldsmith, *Wireless communications*, Cambridge University press, 2005.

[23] J.G. Proakis, *Digital Communications*, McGraw-Hill, 1989.

VITA

Xiaoyu Feng received the B. Eng. degree in Automation Science and Electrical Engineering from Beijing University of Aeronautics and Astronautics, Beijing, China, in 2007. He is currently pursuing the Ph.D. degree in the Department of Electrical and Computer Engineering, Louisiana State University, Baton Rouge. His research interests are in the areas of digital communication and communication theory.